

# Developmentally Regulated and Evolutionarily Conserved Expression of SLITRK1 in Brain Circuits Implicated in Tourette Syndrome

ALTHEA A. STILLMAN,<sup>1</sup> ŽELJKA KRSNIK,<sup>2,3</sup> JINHAO SUN,<sup>2</sup> MLADEN-ROKO RAŠIN,<sup>2,3</sup> MATTHEW W. STATE,<sup>1,5,6</sup> NENAD ŠESTAN,<sup>2,3</sup> AND ANGELIKI LOUVI<sup>2,4,6\*</sup>

<sup>1</sup>Department of Genetics, Yale University School of Medicine, New Haven, Connecticut 06520

<sup>2</sup>Department of Neurobiology, Yale University School of Medicine, New Haven, Connecticut 06520

<sup>3</sup>Kavli Institute of Neuroscience, Yale University School of Medicine, New Haven, Connecticut 06520

<sup>4</sup>Department of Neurosurgery, Yale University School of Medicine, New Haven, Connecticut 06520

<sup>5</sup>Child Study Center, Yale University School of Medicine, New Haven, Connecticut 06520

<sup>6</sup>Program on Neurogenetics, Yale University School of Medicine, New Haven, Connecticut 06520

## ABSTRACT

Tourette syndrome (TS) is an inherited developmental neuropsychiatric disorder characterized by vocal and motor tics. Multiple lines of neurophysiological evidence implicate dysfunction in the corticostriatal-thalamocortical circuits in the etiology of TS. We recently identified rare sequence variants in the *Slit and Trk-like family member 1 (SLITRK1)* gene associated with TS. SLITRK1, a single-pass transmembrane protein, displays similarities to the SLIT family of secreted ligands, which have roles in axonal repulsion and dendritic patterning, but its function and developmental expression remain largely unknown. Here we provide evidence that SLITRK1 has a developmentally regulated expression pattern in projection neurons of the corticostriatal-thalamocortical circuits. SLITRK1 is

further enriched in the somatodendritic compartment and cytoplasmic vesicles of cortical pyramidal neurons in mouse, monkey, and human brain, observations suggestive of an evolutionarily conserved function in mammals. SLITRK1 is transiently expressed in the striosomal/patch compartment of the mammalian striatum and moreover is associated with the direct output pathway; adult striatal expression is confined to cholinergic interneurons. These analyses demonstrate that the expression of SLITRK1 is dynamic and specifically associated with the circuits most commonly implicated in TS and related disorders, suggesting that SLITRK1 contributes to the development of corticostriatal-thalamocortical circuits. *J. Comp. Neurol.* 513:21–37, 2009. © 2008 Wiley-Liss, Inc.

Indexing terms: pyramidal neuron; striatum; cholinergic neuron; dopamine; corticostriatal-thalamocortical circuits

Tourette syndrome (TS) is a potentially debilitating developmental neuropsychiatric syndrome, characterized by chronic vocal and motor tics, affecting as many as 1 in 100 individuals (Hornse et al., 2001; Robertson, 2003; Singer, 2005). Direct and indirect evidence has suggested that the corticostriatal-thalamocortical circuits mediate the symptoms of TS and obsessive compulsive disorder (OCD), a comorbid condition often seen in affected individuals and their families (Berardelli et al., 2003; Singer and Minzer, 2003; Hoekstra et al., 2004; Singer, 2005); however, the molecular and cellular mechanisms of disease have not yet been determined. Both the striatal and the cortical components of the circuit have been investigated; the former has long been considered likely to play a role because of its known association with other movement disorders, and the latter has attracted increasing attention recently as evidence has accumulated supporting cortical dysfunction in affected individuals (Singer, 2005; Harris and Singer, 2006). Several decades of investigation have con-

firmed a substantial genetic contribution to TS (State et al., 2001), but specific causal or risk alleles have been difficult to identify. Based on the available evidence, TS is clearly a

Additional Supporting Information may be found in the online version of this article.

Grant sponsor: National Institutes of Health; Grant number: R01NS054273 (to N.Š.); Grant number: R01NS056276 (to M.W.S.); Grant sponsor: Yale Program on Neurogenetics, Autism Speaks (M.R.R.).

The first two authors contributed equally to this work.

Jinhao Sun's current address is Department of Anatomy, School of Medicine, Shandong University, Jinan, Shandong 250012, People's Republic of China.

\*Correspondence to: Angeliki Louvi, Department of Neurosurgery and Program on Neurogenetics, Yale University School of Medicine, P.O. Box 208082, New Haven, CT 06520-8082. E-mail: angeliki.louvi@yale.edu

Received 14 April 2008; Revised 5 June 2008; Accepted 15 October 2008  
DOI 10.1002/cne.21919

Published online in Wiley InterScience (www.interscience.wiley.com).

genetically heterogeneous disorder, likely involving multiple alleles at different loci. The number of genes and the distributions of common or rare alleles contributing to the TS spectrum disorders have not yet been determined.

We have recently identified *Slit and Trk-like family member 1 (SLITRK1)* as a strong candidate gene for involvement in rare cases of TS spectrum disorders (Abelson et al., 2005). SLITRK proteins are a family of neuronal transmembrane molecules (Aruga and Mikoshiba, 2003; Aruga et al., 2003). Their extracellular domain has homology to the secreted SLIT ligands, which have roles in axonal repulsion and dendritic patterning (Brose et al., 1999; Li et al., 1999; Whitford et al., 2002), whereas the intracellular domain shows similarities to the neurotrophic-responsive tyrosine kinases (TRKs). SLITRK1 is unique among this protein family in that it lacks canonical tyrosine phosphorylation sites in its short cytoplasmic domain. When overexpressed, SLITRK1 enhances unipolar neurite outgrowth in cell lines (Aruga and Mikoshiba, 2003) and dendritic branching in primary pyramidal cortical neurons (Abelson et al., 2005). Preliminary evidence (Aruga and Mikoshiba, 2003; Abelson et al., 2005) has demonstrated that *Slitrk1* is expressed in the embryonic and postnatal mouse brain, including the cortex, thalamus, and basal ganglia, reflecting the neuroanatomical regions most commonly implicated in TS. *Slitrk1*-deficient mice were recently described as displaying elevated anxiety-like behavior, possibly because of noradrenergic abnormalities (Katayama et al., 2008).

Here we demonstrate that the expression of SLITRK1 is developmentally regulated in mouse, monkey, and human brain. SLITRK1 is detected in layer 3, 5, and 6 cortical pyramidal neurons that participate in corticocortical, corticothalamic, and corticostriatal circuits and is moreover associated with the apical dendrite. In the striatum, SLITRK1 expression is high in striosomes/patches during early brain development but significantly diminished later, suggesting a possible role in establishing the corticostriatal circuitry. It is further restricted to striatal projection neurons of the direct pathway. These results confirm developmentally regulated expression of SLITRK1 in the neuroanatomical circuits most commonly implicated in TS and related disorders and offer insights into the potential function(s) of this protein in brain development and pathogenesis.

## MATERIALS AND METHODS

### Mice

Experiments were carried out in accordance with protocols approved by the Institutional Animal Care and Use Committee at Yale University School of Medicine. Adult CD1 mice (older than 3 months) were purchased from Charles River Laboratories (Wilmington, MA). Mouse colonies were maintained at Yale University, in compliance with National Institutes of Health guidelines and with the approval of Yale University Institutional Animal Care and Use Committee. For timed pregnancies, midday of the day of vaginal plug discovery was considered embryonic (E) day 0.5. Mice at embryonic and postnatal stages through adulthood were used. For embryonic stages, pregnant females were anesthetized, and pups at appropriate stages were extracted from the uterus. Embryonic brains were dissected and fixed by immersion in 4% paraformaldehyde (PFA) in phosphate-buffered saline (PBS), pH 7.4.

Mouse pups [postnatal (P) day 0 through P2] were deeply anesthetized on ice, and then the brains were removed and fixed in 4% PFA. At all other stages, mice were anesthetized with injectable anesthetics (100 mg/kg ketamine and 10 mg/kg xylazine) and intracardially perfused with 4% PFA.

### Human and monkey brain specimens

Post-mortem human brain specimens were collected following guidelines on the research use of human brain tissue from the New York State-licensed Human Fetal Tissue Repository at Albert Einstein College of Medicine and the Croatian Institute for Brain Research, University of Zagreb Medical School. Tissues from the Zagreb Neuroembryological Collection were obtained with approval from the Medical Ethical Committee at the University of Zagreb Medical School. For each tissue donation, appropriate written, informed consent and approval were obtained. The study was approved by the Human Investigation Committee at Yale University School of Medicine. Monkey brain specimens were collected from one embryonic (E140) and two adult macaque monkeys (*Macaca mulatta*; rhesus monkey). To obtain the embryo, a caesarean section was performed as previously described (Rakic and Goldman-Rakic, 1985). In short, the pregnant monkey was first sedated with ketamine (3 mg/kg) and atropine sulfate (Lilly; 0.2 mg/kg). A catheter was introduced into the saphenous vein for continuous administration of fluids. Surgery was performed aseptically under halothane-nitrous oxide-oxygen anesthesia. Postoperatively, the animal was administered painkillers, and the wound was periodically cleaned. The animal was monitored until full recovery. The adult monkeys had been retired from a breeding colony in the Department of Neurobiology, in compliance with National Institutes of Health guidelines and with the approval of Yale University Institutional Animal Care and Use Committee.

### In situ hybridization

Mouse brains were removed, postfixed overnight in 30% sucrose/4% PFA, and sectioned in the coronal plane on a Leica sledge cryomicrotome at 36  $\mu\text{m}$  (Leica Microsystems, Wetzlar, Germany). Sections were mounted on slides and processed for nonradioactive in situ hybridization as described previously, with minor modifications (Tole and Patterson, 1995; Grove et al., 1998). An RNA probe complementary to mouse *Slitrk1* (bases 322–1383 of the mouse *Slitrk1* cDNA, NM\_199065) was prepared and labeled with digoxigenin-11-UTP. Sections were analyzed with a Zeiss Stemi dissecting microscope or a Zeiss Axiomager (Zeiss, Oberkochen, Germany) fitted with an AxioCam MRc5 digital camera. Images were captured using AxioVision AC software (Zeiss) and assembled in Adobe Photoshop.

### Antibody characterization

All antibodies used in this study were individually examined following immunostaining of mouse brain sections by confocal microscopy to ensure that the signal appeared specific and was concordant with known information about the protein. Additional information about each antibody is listed in Table 1.

The B-cell CLL/lymphoma 11B (BCL11B) antibody detected two bands of  $\sim 120$  kD molecular weight corresponding to the two splice variants of BCL11B on Western blots of Jurkat cell lysates (manufacturer's technical information) and detected

TABLE 1. Primary Antibodies Used

Antigen	Immunizing antigen	Host species	Source/catalog number	Dilution
B-cell CLL/lymphoma 11B (BCL11B; CTIP2)	GST fusion peptide of the N-terminal region of human CTIP2 (amino acids 1-173)	Rat (monoclonal)	Abcam, Inc. (Cambridge, MA) # ab18465	1:100
Calbindin 2 (CALB2) (Calretinin)	Recombinant human calretinin-22k	Mouse (monoclonal)	Swant (Bellinzona, Switzerland) # 6B3	1:2,000
Choline acetyltransferase (ChAT)	Purified choline acetyltransferase from human placenta	Rabbit (polyclonal)	Millipore (Billerica, MA) # AB143	1:500
D <sub>1</sub> Dopamine Receptor	Synthetic peptide corresponding to amino acids 230-248 of human D <sub>1</sub> dopamine receptor conjugated to KLH	Rabbit (polyclonal)	Sigma-Aldrich (St. Louis, MO) # D6692	1:250
Enkephalin	Synthetic methionine enkephalin conjugated to bovine thyroglobulin with glutaraldehyde	Rabbit (polyclonal)	ImmunoStar, Inc. (Hudson, WI) # 20065	1:500
Forkhead box P2 (FOXP2)	Synthetic peptide (CREIEEPLSEDE) corresponding to amino acids 703-715 of the C-terminus of human FOXP2	Rabbit (polyclonal)	Abcam, Inc. # ab16046	1:150,000
$\gamma$ -Aminobutyric Acid (GABA)	GABA-BSA	Rabbit (polyclonal)	Sigma-Aldrich # A2052	1:2,000
Glial Fibrillary Acidic Protein (GFAP)	Purified glial fibrillary acidic protein from human brain	Guinea pig (polyclonal)	Advanced ImmunoChemical, Inc. (Long Beach, CA) #31223	1:500
Giantin	N-terminal region of human giantin corresponding to amino acids 1-469	Rabbit (polyclonal)	Covance, Inc. (Princeton, NJ) # PRB-114C	1:1,000
MAP2	Rat brain microtubule-associated proteins (MAPs) and isotype was then determined	Mouse (monoclonal)	Sigma-Aldrich # M4403	1:1,000
$\mu$ opioid receptor	Synthetic peptide corresponding to amino acids 384-398 of rat MOR1	Rabbit (polyclonal)	ImmunoStar, Inc. # 24216	1:250
Nitric oxide synthase 1, neuronal (NOS1; nNOS)	Synthetic peptide corresponding to amino acids 134-148 of human nNOS conjugated to KLH	Rabbit (polyclonal)	ImmunoStar, Inc. # 24431	1:500
Parvalbumin	Purified parvalbumin from carp muscle	Mouse (monoclonal)	Swant # 235	1:500
Rab5	Synthetic peptide PKNEPQNPGANSARGR corresponding to amino acids 182-197 of human Rab5 conjugated to KLH	Rabbit (polyclonal)	Abcam, Inc. # ab13253	1:1,000
Rab11	Synthetic peptide corresponding to amino acids 130-216 of human Rab11	Rabbit (polyclonal)	Santa Cruz Biotechnology (Santa Cruz, CA) # sc-9020	1:100
Slitrk1	NS0-derived rhSLITRK1 extracellular domain (amino acids 16-616)	Goat (polyclonal)	R&D Systems (Minneapolis, MN) # AF3009	1:200 (IF) 1:1,000 (WB)
SMI-32	Homogenized rat hypothalamii; subsequently determined to recognize non-phosphorelated epitopes on the neurofilament heavy chain	Mouse (monoclonal)	Covance, Inc. # SMI-32R	1:1,000
Substance P	Substance P conjugated to KLH with carbodiimide	Rabbit (polyclonal)	ImmunoStar, Inc. # 20064	1:500

the same two bands on Western blots of lysates of HEK293T cells transiently transfected with an expression vector encoding FLAG-CTIP2 and immunoprecipitated with an anti-FLAG antibody (Topark-Ngarm et al., 2006). This antibody stained a pattern of cellular morphology and distribution in mouse cortical sections identical to that in previous reports (Rašin et al., 2007; Britanova et al., 2008).

The calbindin 2 (CALB2; calretinin-22k) antibody recognized a common epitope for both calretinin and calretinin-22k (a region between EF-hand domains III and IV) on Western blots of mouse and rat brain extracts and dot blots (Zimmermann and Schwaller, 2002) and stained a pattern of cellular morphology and distribution in mouse brain sections identical to that in previous reports (Brandt et al., 2003) and to the authors' unpublished observations.

The choline acetyltransferase (ChAT) antiserum specifically recognized a band of 68 kD m.w. in the ammonium sulfate fraction of placental proteins supplemented with affinity-purified placental ChAT but not in that fraction alone (Bruce et al., 1985) and immunoprecipitated a 68-kD protein that displayed ChAT enzymatic activity from brain and placenta protein extracts; it also precipitated a 27-kD protein that is coexpressed with ChAT but lacks ChAT activity in some cholinergic neurons of the central nervous system (manufacturer's technical information). This antiserum stained cholinergic neurons in rat cerebral cortex (Lysakowski et al., 1989). The authors independently assessed the staining pattern in

mouse basal ganglia sections and found it identical to previous reports (Gabriel and Witkovsky, 1998); furthermore, preincubation with recombinant rat ChAT protein abolished staining of large striatal neurons with morphology characteristic of cholinergic interneurons.

The D<sub>1</sub> dopamine receptor antiserum specifically recognized a band of ~50 kD m.w. on Western blots of membrane protein extracts from rat striatum and cerebellum (manufacturer's technical information); the authors independently assessed the staining pattern in mouse brain sections and found it identical to that in previous reports (Levey et al., 1993; Yung et al., 1995).

The enkephalin antiserum was tested for specificity by immunohistochemistry; staining was eliminated by preincubation with the immunizing peptide. The antiserum stained a pattern of cellular morphology and distribution in mouse brain sections that is identical to that in previous reports (Holt and Newman, 2004).

The forkhead box P2 (FOXP2) antiserum recognized a band of 80 kD m.w. on Western blots of human 293T cell lysates (manufacturer's technical information); in chromatin immunoprecipitation assays, this antiserum identified DNA binding sites also identified with a different FOXP2 antiserum raised in rabbits immunized with the synthetic peptide EDLNGSLDHID-SNG (C-terminal region of FOXP2) conjugated to KLH (Spiteri et al., 2007). The antiserum stained a pattern of cellular mor-

phology and distribution in mouse brain sections identical to that in previous reports (Rašin et al., 2007; Fujita et al., 2008).

The  $\gamma$ -aminobutyric acid (GABA) antiserum showed positive binding with GABA and GABA-KLH in dot blot assays and negative binding with bovine serum albumin (BSA; manufacturer's technical information) and stained a pattern of cellular morphology and distribution in mouse brain sections identical to that in previous reports (Ang et al., 2003; Lee et al., 2006).

The glial fibrillary acidic protein (GFAP) antiserum detected a band of 43–45 kD m.w. on Western blots of human brain and spinal cord lysates, corresponding to the predicted molecular weight of GFAP (manufacturer's technical information) and stained a pattern of cellular morphology and distribution in mouse brain sections identical to that in previous reports in rat (Capani et al., 2001; Lai et al., 2003).

The giantin antiserum detected a band of ~400 kD m.w. on Western blots of mammalian cell lines (including human intestine, lung fibroblasts, and liver and rat and mouse fibroblasts) and by immunostaining (manufacturer's technical information) and stained a pattern of cellular morphology and distribution in mouse brain sections identical to that in previous reports (Ren et al., 2003; Zheng et al., 2007).

The MAP2 antibody reacted with all known forms of MAP2 (MAP2a–c) on Western blots of combined newborn and adult rat brain lysates, in which it detected two bands of 280 kD m.w. (corresponding to the similarly sized MAP2a and MAP2b) and 70 kD m.w. (MAP2c) and on immunohistochemistry with no cross-reactivity with other MAPs or tubulin (manufacturer's technical information) and stained a pattern of cellular morphology and distribution in mouse brain sections identical to that in previous reports on rat telencephalon (Fujimori et al., 2002).

The  $\mu$ -opioid receptor antiserum detected a band of about 60 kD m.w. on Western blots, corresponding to the predicted molecular weight of  $\mu$ -opioid receptor, and provided specific staining in trigeminal ganglion neurons (Berg et al., 2007). Preabsorption of the antibody with the immunizing peptide blocked signal in immunolabeling (manufacturer's technical information).

The nitric oxide synthase 1, neuronal (NOS1; nNOS) antiserum recognized a band of 155 kD m.w. on Western blots of rat brain lysates, and immunolabeling was abolished with preabsorption of the corresponding immunizing peptide (manufacturer's technical information). The antiserum stained a pattern of cellular morphology and distribution in mouse brain identical to that in previous reports (Pla et al., 2006; Fuentes-Santamaria et al., 2008).

The parvalbumin antibody specifically recognized a spot of 12 kD m.w. on two-dimensional gels of rat cerebellar protein extracts, which is identical to purified parvalbumin; the same spot binds  $\text{Ca}^{2+}$ , and, furthermore, the antibody stained Purkinje cells in the cerebellum (Celio et al., 1988) and stained a pattern of cellular morphology and distribution in mouse brain sections identical to that in previous reports (Fazzari et al., 2007).

The Rab5 antiserum recognized a band of 26 kD m.w. (and occasionally a second, potentially nonspecific band) on Western blots of rat and mouse brain lysates and transfected Rab5 protein in cells by immunocytochemistry (manufacturer's technical information) and stained a pattern of cellular distribution in mouse brain identical to that in previous reports

(Cataldo et al., 2003) and to the authors' unpublished observations.

The Rab11 antiserum detected a single band of about 24 kD m.w. on Western blots of human platelet and mouse liver extracts (manufacturer's technical information; Becker and Hannun, 2003) and stained a pattern of cellular morphology and distribution in mouse brain identical to that in previous reports (Rašin et al., 2007).

The Slitrk1 antiserum recognized human SLITRK1 in direct ELISA assays and Western blots (manufacturer's technical information). Its specificity was further examined on Western blots of mouse and human brain protein extracts in the absence or presence of the immunizing peptide (recombinant human SLITRK1 extracellular domain; R&D Systems, Minneapolis, MN; No. 3009-SK) and of protein lysates from Cos7 cells transfected with a FLAG-tagged human SLITRK1 expression plasmid (Supp. Info. Fig. 1). In situ hybridization results presented herein, as well as our unpublished data, identified mRNA expression patterns identical to those revealed by immunostaining with this antibody.

The SMI-32 antibody recognized two bands (200 and 180 kD) that merge into a single NFH line on two-dimensional blots of rat brain homogenates and found to be specific for non-phosphorylated neurofilament H (Goldstein et al., 1987) and stained a pattern of cellular morphology and distribution in mouse brain identical to that in previous reports (Fernandez-Chacon et al., 2004).

The substance P antiserum specifically stained neurons in substantia nigra and spinal cord; staining was abolished by preincubation with the immunizing peptide (manufacturer's technical information). The antiserum stained a pattern of cellular morphology and distribution in mouse brain identical to that in previous reports (Morgado-Valle and Feldman, 2004; Sun and Chen, 2007).

### Immunohistochemistry

Embryonic, postnatal, and adult mouse brains were collected and fixed as described above, cryoprotected in 30% sucrose in PBS, sectioned at 40  $\mu\text{m}$  using a sledge microtome in the coronal plane, and processed freely floating. Fetal and adult monkey and human brains were fixed in 4% PFA, cryoprotected in 30% sucrose, frozen by immersion in 2-methylbutane, and stored at  $-80^\circ\text{C}$ . Blocks were sectioned frozen at 60  $\mu\text{m}$  with a cryostat and processed freely floating.

For diaminobenzidine (DAB) staining with the goat anti-SLITRK1 antibody, sections of embryonic, postnatal, or adult mouse and of fetal or adult monkey and human brain were treated with 1%  $\text{H}_2\text{O}_2$ ; washed in PBS; and preincubated in blocking solution (BS) containing 5% normal donkey serum (Jackson ImmunoResearch Laboratories, West Grove, PA), 1% BSA, 0.1% glycine, 0.1% L-lysine, and 0.03% Triton X-100. The sections were then incubated with anti-SLITRK1 antibody for 36 hours at  $4^\circ\text{C}$ . After washes with PBS, the sections were incubated with secondary antibody [donkey anti-goat Biotin-SP (Jackson ImmunoResearch Laboratories; 1:250 dilution)] for 2 hours at room temperature, washed in PBS, and then incubated with Vectastain ABC Elite solution (Vector, Burlingame, CA) for 2 hours. Sections were developed with 0.05% DAB (pH 7.4), 0.2% glucose, 0.01% nickel ammonium sulfate, 0.04% ammonium chloride, and 8  $\mu\text{g}/\text{ml}$  glucose oxidase and then rinsed, mounted onto glass slides, allowed to dry, dehydrated, and coverslipped. For double staining with

the goat anti-SLITRK1 and mouse anti-ChAT antibodies, adult mouse, monkey, and human brain sections were first incubated with the anti-SLITRK1 antibody and processed for DAB staining as described, followed by incubation with the anti-ChAT antibody for 36 hours at 4°C, washes in PBS, incubation with secondary antibody [horseradish peroxidase (HRP)-conjugated donkey anti-mouse IgG (Vector, 1:200 dilution)] for 2 hours, washes in PBS, and then incubation with Vectastain ABC peroxidase solution (Vector) for 2 hours. Sections were developed using Nova Red peroxidase substrate (Vector) and then rinsed, mounted onto glass slides, allowed to dry, dehydrated, and coverslipped.

For immunofluorescence, mouse brain sections were placed in BS without H<sub>2</sub>O<sub>2</sub> treatment and then incubated in primary antibodies for 36 hours at 4°C. Secondary antibodies were all highly cross-absorbed, raised in donkey, conjugated to cyanine 2 (Cy2) or Cy3 (Jackson ImmunoResearch Laboratories), and used at 1:250 dilution in BS without Triton X-100 for 2 hours at room temperature. The sections were mounted, coverslipped with DAPI-containing Vectashield (Vector), and analyzed with a confocal microscope (Zeiss).

### Image capture and analysis

Tissue sections were photographed by using a Zeiss AxioImager fitted with a Zeiss AxioCam MRc5 digital camera. Images were captured by using AxioVision AC software (Zeiss) and assembled in Adobe Photoshop. Some images were modified to adjust contrast (see Fig. 9). For confocal microscopy, single optical and z-stack images were collected on a Zeiss LSM 510 laser-scanning microscope and assembled in Adobe Photoshop.

### Western blotting

Adult human brain protein extracts (Human Brain Protein Medley) were obtained from Clontech Laboratories (Mountain View, CA). Adult mouse brains were dissected and homogenized in lysis buffer [10 mM Tris, 200 mM NaCl, 1 mM EDTA (pH 7.4), 2% SDS] containing protease inhibitors (Roche Applied Science, Indianapolis, IN). Fifty-microgram protein samples were analyzed via SDS-PAGE under reducing conditions with a 4–15% gradient polyacrylamide gel. Western blotting was performed with anti-SLITRK1 antibody (dilution 1:1,000) and HRP-conjugated donkey anti-goat secondary antibody (dilution 1:5,000); the signal was detected by using a chemiluminescence system (ECL Western Blotting Detection system; GE Healthcare Bio-Sciences Corp., Piscataway, NJ). The blots were stripped with 2% SDS and  $\beta$ -mercaptoethanol and reprobed with HRP-conjugated anti- $\beta$ -actin (1:5,000; Sigma, St. Louis, MO) for loading control. For peptide competition analyses, the primary goat anti-SLITRK1 antibody was preabsorbed at a 1:5 ratio with the corresponding immunizing peptide (R&D Systems) at room temperature for 2 hours prior to application for both immunostaining and Western blot assays.

### Immunogold labeling and electron microscopy

Two protocols were used. For the first, adult mouse and rhesus monkey brain tissue was fixed in 4% PFA with 0.3% glutaraldehyde (Electron Microscopy Sciences, Hatfield, PA) and sectioned with a vibratome at 70  $\mu$ m. Sections were treated with 0.3% H<sub>2</sub>O<sub>2</sub> in PBS, washed in PBS, preincubated in BS (see above), and then incubated with goat anti-SLITRK1 antibody (1:200) for 36 hours. After washing, the sections were

incubated in BS with 0.1% gelatin (GE Healthcare Bio-Sciences Corp.) for 1 hour. Secondary antibody conjugated to 6- or 12-nm gold particles (1:40; Jackson ImmunoResearch Laboratories) was applied overnight at 4°C. After washing and a 10-minute fixation in 2% glutaraldehyde and further washes in PBS and dH<sub>2</sub>O, silver intensification was applied as recommended by the manufacturer (Aurion). After gold immunostaining, sections were washed for 4 hours in phosphate buffer (PB) and then dehydrated as follows: 2  $\times$  1 minutes in 50% EtOH, 45 minutes in 1% uranyl acetate in 70% EtOH, 2  $\times$  1 minutes each in 70%, 90%, and 100% EtOH and in propylene oxide. Sections were then embedded overnight in Durcupan (Sigma-Aldrich), mounted on microscopy slides, and kept at 60°C overnight. SLITRK1-immunopositive regions were identified by light microscopy, reembedded, sectioned ultrathin (60 nm), collected on single whole copper grids (Electron Microscopy Sciences), and contrasted with lead citrate for 2–4 minutes before EM analysis. EM images were captured with a Multiscan 792 digital camera (Gatan, Pleasanton, CA). Representative immunoelectron micrographs are shown in Figure 7E,F. For the second protocol, adult mouse brain tissue was fixed in 4% PFA/0.2% glutaraldehyde in 0.25 M HEPES, pH 7.4, and postfixed overnight in the same solution. Small blocks of tissue were then embedded in gelatin, cryoprotected in sucrose, rapidly frozen in liquid N<sub>2</sub>, and sectioned ultrathin on a Leica cryomicrotome (Leica Microsystems) at 60–80 nm. Grids were immunolabeled with goat anti-SLITRK1 antibody (1:20 and 1:100) for 30 minutes at room temperature, washed in PBS, labeled with secondary antibody, washed in PBS, labeled with Protein A-gold for 30 minutes at room temperature, washed in PBS, postfixed in 1% glutaraldehyde for 5 minutes, washed in distilled water, stained with 2% neutral uranyl acetate for 10 minutes, washed briefly in water, and rinsed with 1.8% methylcellulose/0.5% uranyl acetate. Samples were examined on a Philips Tecnai 12 BioTWIN electron microscope (FEI Co.). Images were captured digitally with a CCD camera (Morada; Soft Imaging Systems). Representative immunoelectron micrographs are shown in Figure 7G–J.

### Retrograde tracing

Adult mouse brains were stereotaxically injected with the retrograde tracers (Retro Beads; Lumafuor, Naples, FL) or BDA-3k (dextran-3000 MW conjugated to tetramethylrhodamine; Molecular Probes, Eugene, OR) into the contralateral neocortex and ipsilateral caudate-putamen (i.e., striatum) and thalamus (lateral posterior nucleus). After 7 days, the animals were killed, and brains were processed for immunofluorescence with anti-SLITRK1 antibody.

## RESULTS

### SLITRK1 is developmentally regulated in the corticostriatal-thalamocortical circuits

We studied *Slitrk1* mRNA expression in the embryonic and postnatal mouse brain using in situ hybridization and placing emphasis on corticostriatal-thalamocortical pathway components given their likely role in the pathophysiology of TS. *Slitrk1* mRNA was first detected at E8.75 in a restricted domain of the ventral neural tube at the level of the midbrain/hindbrain boundary. This expression domain was maintained and spread both anteriorly and posteriorly over the next 2

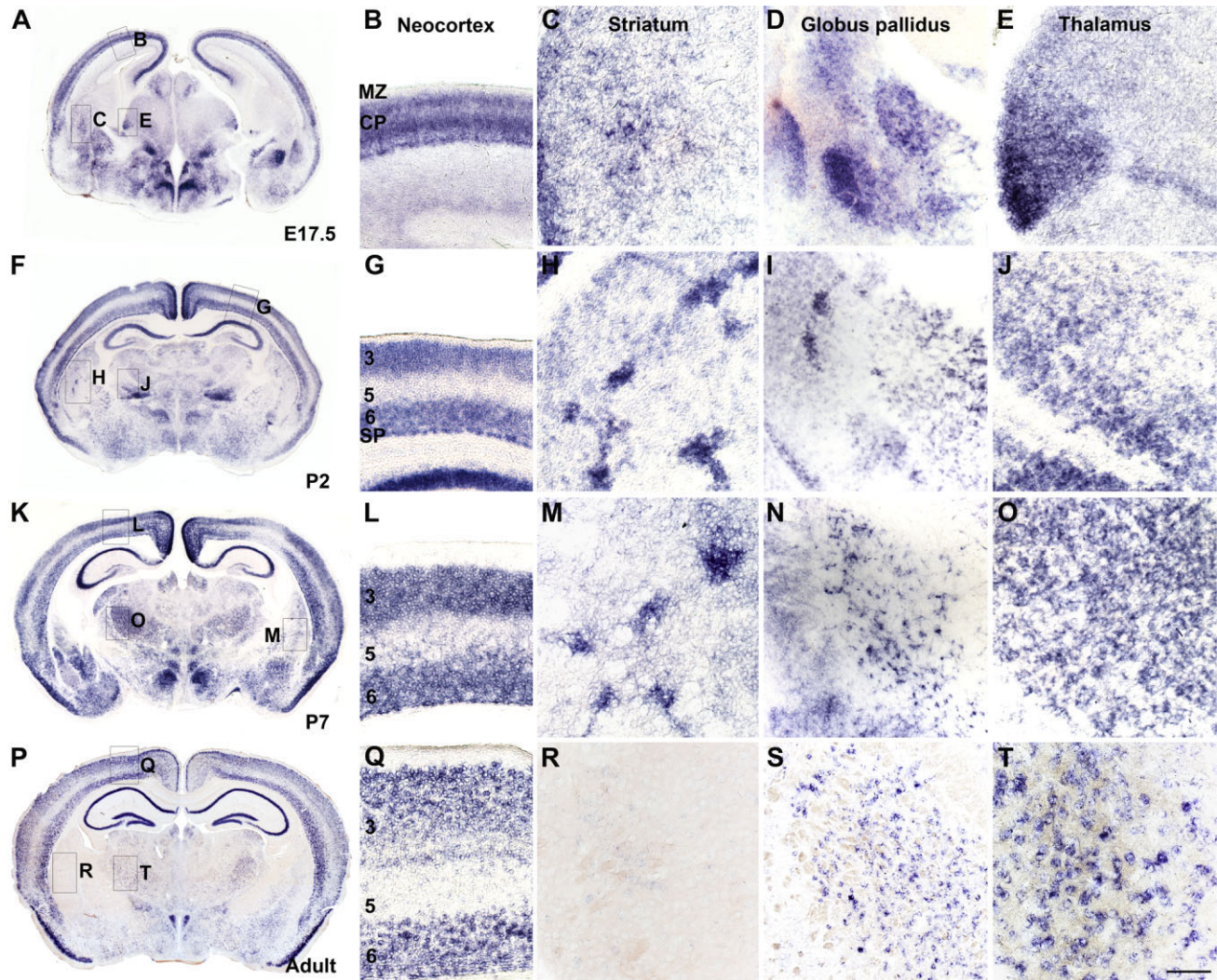


**Figure 1.** *Slitrk1* mRNA expression in mouse brain. **A,F,K,P:** Whole views of coronal sections of E17.5, P2, P7, and adult brain assayed via in situ hybridization with a digoxigenin-labeled antisense riboprobe. Boxes indicate regions where higher magnification images were taken. **B,G,L,Q:** Magnified views of the neocortex. *Slitrk1* is highly expressed in prospective and mature cortical layers 3, 5, and 6, which contain projection neurons. **C,H,M,R:** Magnified views of the striatum. *Slitrk1* is widely expressed in the embryonic striatum and becomes compartmentalized at early postnatal stages. **R:** *Slitrk1* expression is virtually undetectable in adult striatum, with only sparse cells expressing *Slitrk1* mRNA. **D,I,N,S:** Magnified views of the globus pallidus. *Slitrk1* is expressed in the developing and adult globus pallidus. **E,J,O,T:** Magnified views of the thalamus. *Slitrk1* is expressed broadly in the developing thalamus and becomes more refined to subsets of prospective thalamic nuclei, including the midline and intralaminar nuclei; mediodorsal, laterodorsal, and parafascicular nuclei; and ventral lateral and ventral posterior complex (see Results). CP, cortical plate; MZ, marginal zone; 3, 5, 6, cortical layers 3, 5, and 6; SP, subplate. Scale bar = 200  $\mu\text{m}$  in T (applies to B–E,G–J,L–O,Q–T).

days, so that, by E11.5, *Slitrk1* mRNA was detected in the ventral midencephalon/diencephalon, telencephalon, and hindbrain (data not shown). In the developing neocortex, by E14.5, *Slitrk1* expression was confined to the cortical plate but was absent from the proliferating progenitors in the ventricular zone. Low levels of expression were evident in the intermediate zone, and this pattern was maintained in late embryogenesis (Fig. 1A,B). Embryonic expression was also prominent in the developing septal area, basal ganglia (Fig. 1A,C), globus pallidus (Fig. 1A,D), thalamus (Fig. 1A,E), hypothalamus, midbrain, mesopontine area, cerebellum, medulla, and spinal cord (data not shown).

In the developing and adult cortex, *Slitrk1* was highly expressed in prospective and mature cortical layers 3, 5, and 6, which contain pyramidal projection neurons (Fig. 1F,G,K,L,P,Q). In the developing dorsal and ventral thalamus, *Slitrk1* was expressed broadly (Fig. 1A,E) and became gradually refined to subsets of prospective nuclei that included, at postnatal stages, the reticular nucleus; midline and intralaminar nuclei; mediodorsal, laterodorsal, and parafascicular nuclei; and ventral lateral and ventral posterior complex; expression in the ventral lateral and ventral anterior nuclei diminishes in the adult (Fig. 1F,J,K,O,P,T). In the striatum, *Slitrk1* expression changed significantly during development. Initially dif-

fuse, it became compartmentalized with a patchy distribution at P2 (Fig. 1H), remaining particularly prominent through P7 (Fig. 1A,C,F,H,K,M), and then decreased markedly, with only a few striatal neurons showing any evidence of expression at P14; *Slitrk1* mRNA was undetectable by P21 and into adulthood in all but a few neurons (Fig. 1P,R, and data not shown). *Slitrk1* mRNA was also present in the nucleus accumbens until P21 but not in the adult; in the globus pallidus and the substantia nigra pars compacta, expression was detected throughout development and into adulthood (Fig. 1A,D,F,I,K,N,P,S, and data not shown).

We next examined the distribution of the SLITRK1 protein by immunohistochemistry with a commercially available antibody raised against the extracellular domain of human SLITRK1 (see Materials and Methods). Consistently with our *in situ* hybridization findings, we detected SLITRK1 in the cortical plate in future layers 3, 5, and 6 (Fig. 2A); this pattern was elaborated postnatally and maintained through adulthood (Fig. 2D,G,J). SLITRK1 was confined to the somatodendritic compartment of cortical pyramidal neurons, but its relative distribution evolved as development proceeded. In embryonic and early postnatal cortex, SLITRK1 was expressed primarily in apical dendrites (Fig. 2B,E), including the dendritic terminal tufts in the marginal zone; low levels of protein were also detected in the cell body during this period. A shift in expression from the apical dendrites toward the neuronal cell body was evident by P7, where it was primarily confined in the adult, outlining a distinct pyramidal cell shape (Fig. 2H,K) and appearing in an asymmetric, or polarized, pattern within the cell; low levels of expression persisted in the apical dendrites. Protein distribution in the striatum was in accordance with the mRNA expression profile: although diffuse in embryogenesis (Fig. 2C), SLITRK1 appeared compartmentalized in the neonatal striatum (Fig. 2F), assuming a patch-like distribution, especially evident at early postnatal stages (Fig. 2I). After the second postnatal week, expression levels diminished significantly, and, in adult mouse striatum, only a few cells appeared to sustain SLITRK1 expression (Fig. 2L). SLITRK1 expression was further detected in the adult globus pallidus, subthalamic nucleus, and substantia nigra pars compacta (Fig. 3A,B,D–F).

Taken together, these observations demonstrate that SLITRK1 is developmentally regulated. In the cortex, the balance of expression in the somatodendritic compartment shifts from primarily dendritic early to mainly somatic postnatally, possibly reflecting a role in dendritic maturation; in the striatum, SLITRK1 is detected in a specific developmental time window coinciding with the establishment and elaboration of the corticostriatal circuit and is subsequently down-regulated. In the thalamus, SLITRK1 is detected in sensory, association, nonspecific, and motor nuclei, implying its presence in thalamocortical neurons.

### SLITRK1 expression in cortex and striatum is conserved across mammalian species

We further examined SLITRK1 protein distribution in both fetal and adult rhesus monkey as well as human brain and found many similarities to what was seen in mouse, suggesting a conserved function of the protein. In the neocortex at fetal stages, expression was detected in apical dendrites (Fig. 4A,B,G,H), whereas, in adults, SLITRK1 appeared localized in the cell body of pyramidal neurons, in addition to the apical

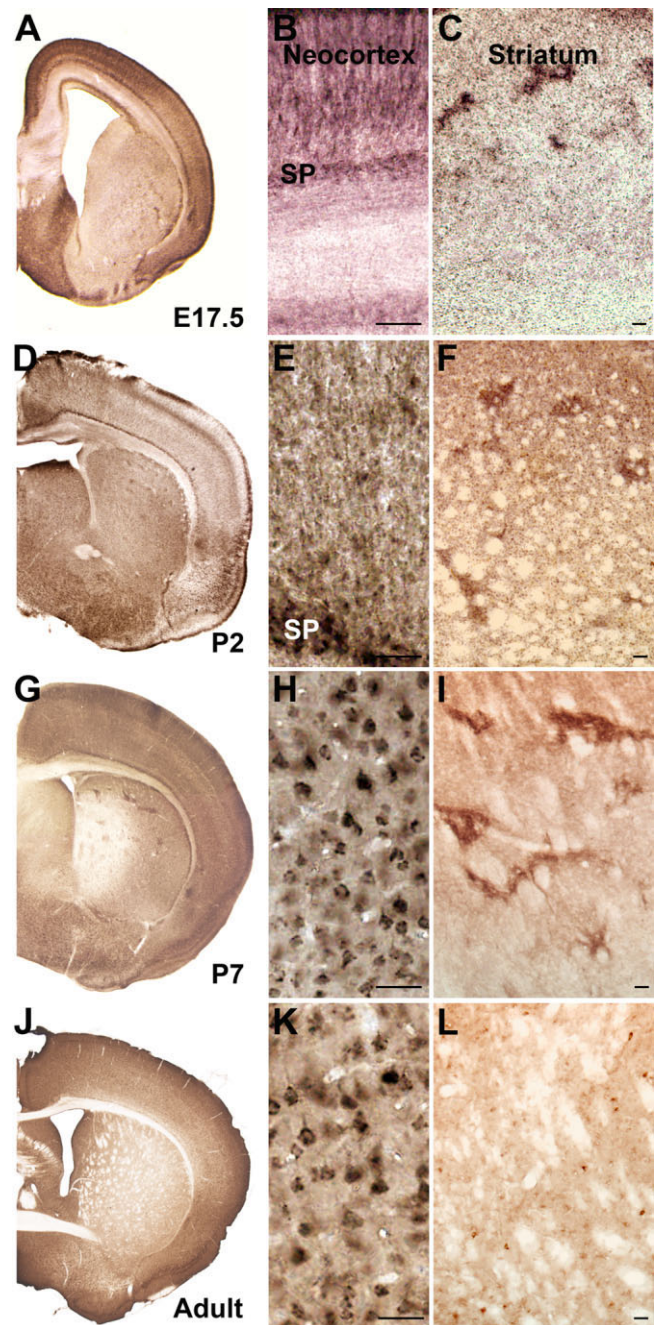


**Figure 2.** SLITRK1 protein expression in mouse brain. **A,D,G,J:** Right coronal hemisection views of E17.5, P2, P7, and adult brain immunostained with an antibody against the extracellular domain of SLITRK1. **B,E:** In late embryonic and early postnatal stages, SLITRK1 is predominantly expressed in apical dendrites. **H,K:** At later postnatal stages and in adult, SLITRK1 is localized predominantly to the cell body outlining a pyramidal shape. **C,F,I:** SLITRK1 is found in patch-like regions in the striatum. **L:** SLITRK1 expression is virtually undetectable in adult striatum, with only a few cells maintaining expression. SP, subplate. Scale bars = 25  $\mu$ m in B,E,H,K; 100  $\mu$ m in C,F,I,L.

dendrites (Fig. 4D,E,J,K). In both species, SLITRK1 was expressed mainly in layers 3, 5, and 6, with little or no staining detected in layers 1 and 2.

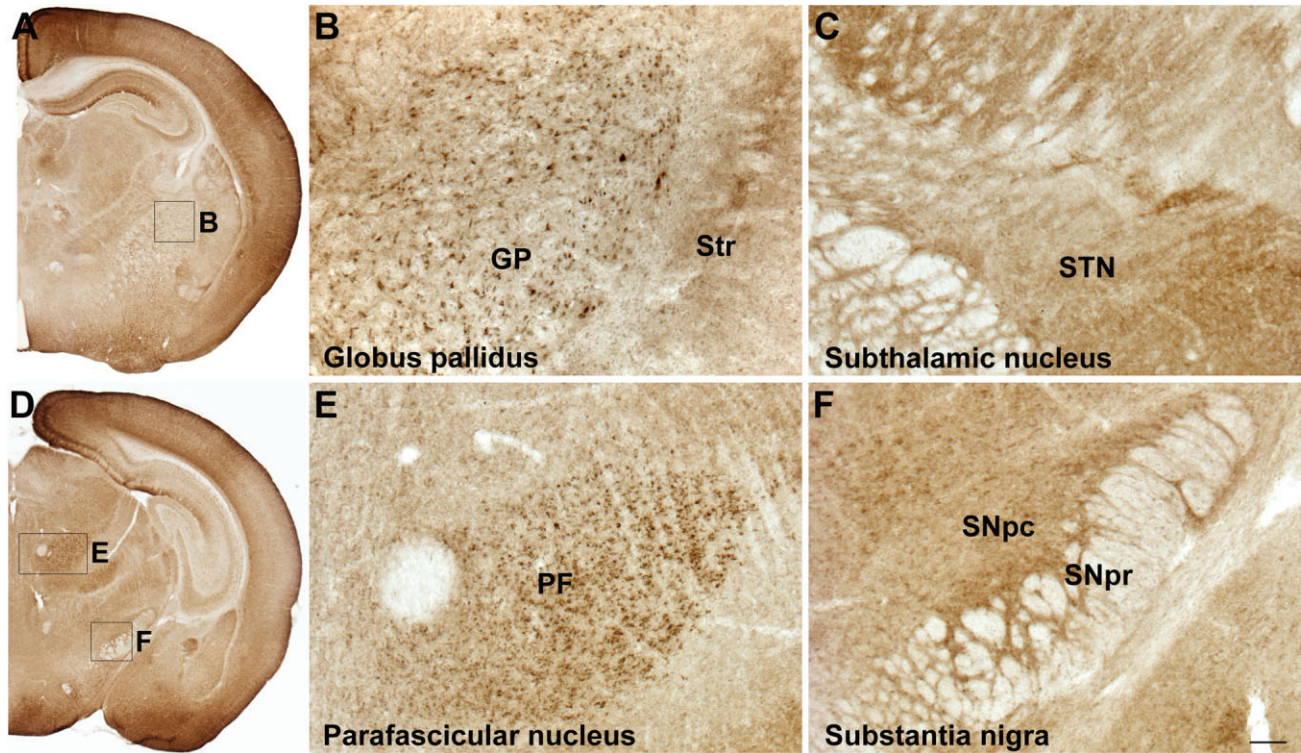


**Figure 3.** SLITRK1 protein expression in thalamus, globus pallidus, and substantia nigra in postnatal mouse brain. Immunolocalization of SLITRK1 with DAB staining. **A,D:** SLITRK1 immunostaining on coronal hemisections of a P7 mouse brain. Boxes indicate regions where higher magnification images were taken. **B,E:** SLITRK1 is highly expressed in the globus pallidus (B) and the thalamic parafascicular nucleus (E). **C,F:** SLITRK1 is not present in the subthalamic nucleus (C) or the substantia nigra pars reticulata (F); it is, however, expressed in the substantia nigra pars compacta (F). GP, globus pallidus; Str, striatum; STN, subthalamic nucleus; PF, parafascicular nucleus; SNpc, substantia nigra pars compacta; SNpr, substantia nigra pars reticulata. Scale bar = 200  $\mu\text{m}$  in F (applies to B,C,E,F).

As in mouse, in fetal monkey and human striatum SLITRK1 protein distribution was compartmentalized in structures reminiscent of striosomes (Fig. 4C,I); with the exception of a few cells, the protein was undetectable in the adult striatum in both species (Fig. 4F,L), which is consistent with our observations in mouse. Thus, for striatum, we also observed similar developmental regulation of SLITRK1 expression in all three mammalian species examined, with the window of expression coinciding with the establishment and elaboration of cortico-striatal connections.

### SLITRK1 is restricted to cortical projection neurons

To characterize further the cortical projection neurons that express SLITRK1, we performed colocalization studies with cell-type-specific markers in P7 mouse cortex. SLITRK1 colocalized with SMI32, a marker of pyramidal neurons with long axonal projections (Campbell and Morrison, 1989; Fig. 5A). Within layer 5, SLITRK1 was expressed in all neurons expressing BCL11B/CTIP2 (Fig. 5B), a transcription factor specific to corticospinal motor neurons and corticotectal neurons (Arlotta et al., 2005). SLITRK1 also colocalized with FOXP2, a forkhead transcription factor involved in the development of human neuronal circuits underlying speech and language (Lai et al., 2001) that is confined to subcortical projection neurons residing predominantly in layer 6 and sparsely in layer 5 (Fer-

land et al., 2003; Fig. 5C). All FOXP2-positive neurons in both layers contained SLITRK1. We further observed partial colocalization of SLITRK1 with the  $D_1$  dopamine receptor (Fig. 5D). On the other hand, interneuron-specific markers revealed no colocalization in the cortex: SLITRK1 was absent from GABAergic interneurons and other interneuron subtypes expressing nitric oxide synthase (NOS), parvalbumin (PVALB), or CALB2/calretinin (Fig. 5E–H). Finally, there was no overlap of SLITRK1 with the astroglial marker GFAP (Fig. 5I).

To determine the projection targets of SLITRK1-expressing cortical neurons, we combined retrograde axonal tracing using fluorescent microspheres (Retro Beads) or BDA-3k with anti-SLITRK1 immunofluorescence. In adult mouse cortex, SLITRK1 protein was detected in retrogradely labeled neurons with axonal projections to the contralateral cortex, ipsilateral striatum, and thalamus (Fig. 6A–C, and data not shown), demonstrating that SLITRK1 is selectively expressed in the cortical projection neurons that make up the corticostriatal-thalamocortical circuitry.

### SLITRK1 subcellular localization in cortical neurons

We examined the subcellular localization of SLITRK1 in the cerebral cortex of adult mouse and rhesus monkey by using immunoelectron microscopy. In both species, we detected SLITRK1 in neuronal dendrites, the periphery of the Golgi

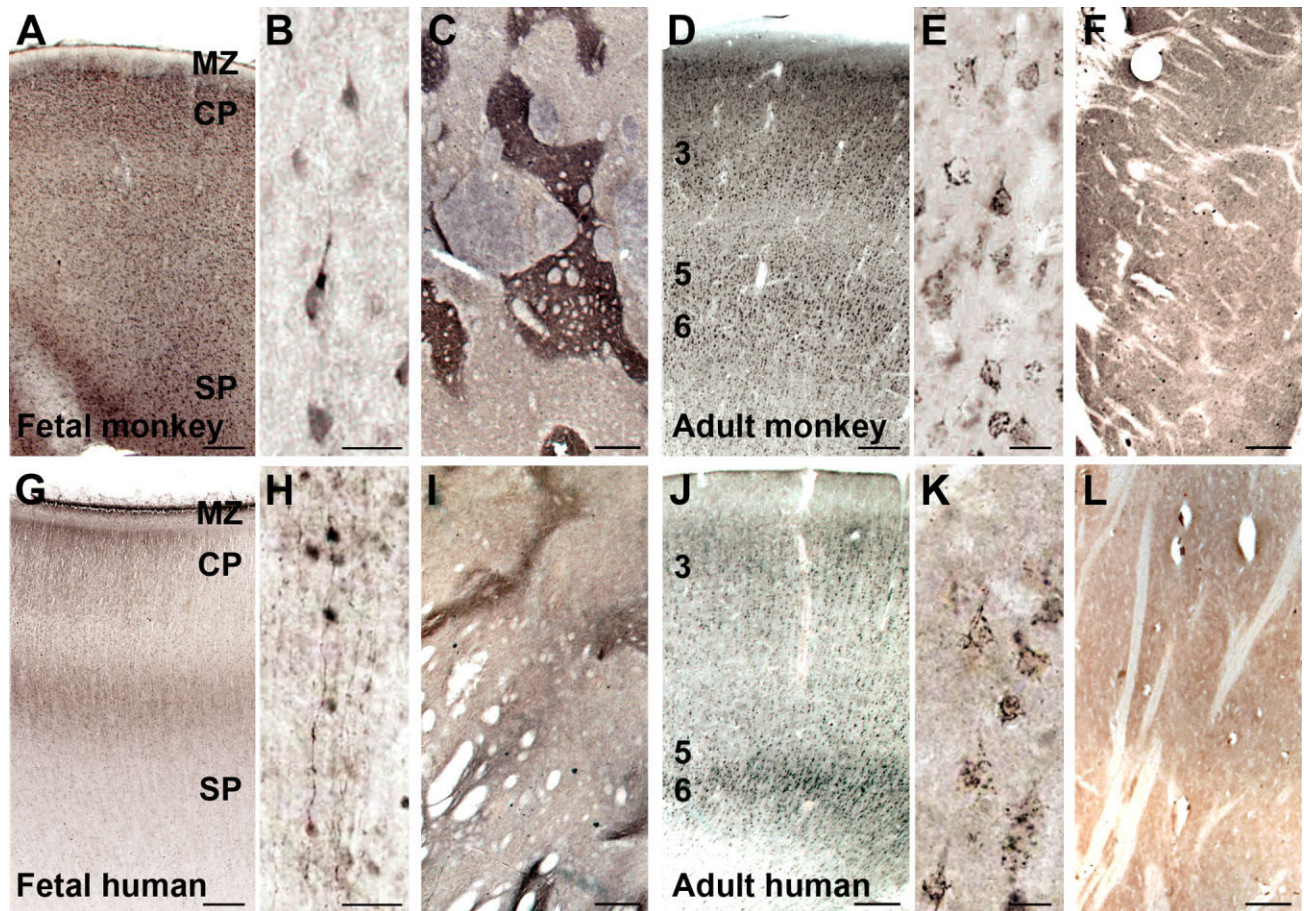


Figure 4.

SLITRK1 protein expression in fetal and adult rhesus monkey and human brain. Immunolocalization of SLITRK1 with DAB staining. **A,D,G,J:** In monkey, as in human, SLITRK1 is expressed in prospective and mature cortical layers 3, 5, and 6 in both fetal (**A,G**) and adult (**D,J**) stages. **B,H:** SLITRK1 is expressed in cortical apical dendrites in fetal monkey and human brain. **E,K:** In adult monkey and human brain, SLITRK1 localization shifts toward the cell body of cortical pyramidal neurons. **C,I:** In fetal monkey and human striatum, SLITRK1 is highly expressed in striosomes. **F,L:** In adult monkey and human striatum, expression is significantly diminished, with no real presence in striosomes. CP, cortical plate; MZ, marginal zone; SP, subplate; 3, 5, 6, cortical layers 3, 5, and 6. Scale bars = 1 mm in **A,C,D,F,G,I,J,L**; 100  $\mu\text{m}$  in **B,E,H,K**.

apparatus, and various cytoplasmic vesicles, including early and late endosomes. SLITRK1 was absent from the nucleus, mitochondria, and rough endoplasmic reticulum (rER; Fig. 7E–J). To confirm the immuno-EM findings, we performed immunofluorescence analyses and confocal microscopy in mouse cerebral cortex at P7 with markers specific to subcellular compartments. SLITRK1 colocalized with the dendritic marker microtubule-associated protein 2 (MAP2; Garner et al., 1988; Fig. 7D) but not with the axonal microtubule-associated protein tau (Dotti et al., 1987; not shown). Within the endocytic pathway, SLITRK1 was found in some early endosomes, colocalizing with RAB5 (Fig. 7A), but in very few recycling endosomes, identified by RAB11 immunoreactivity (Grosshans et al., 2006; Fig. 7B). Additionally, SLITRK1 colocalized with giantin, an integral component of the Golgi apparatus membrane (Linstedt and Hauri, 1993; Fig. 7C).

#### SLITRK1 is confined to the striosomes and the direct pathway

Our in situ hybridization and immunostaining results suggested that *Slitrk1* mRNA and SLITRK1 protein in the striatum

were compartmentalized. Consequently, we used cell-type-specific markers to characterize SLITRK1-expressing cells in mouse striatum at P7. SLITRK1-positive cells expressed the  $\mu$ -opiate receptor, which is greatly enriched in the striosomes (Herkenham and Pert, 1981; Fig. 8A–C). Additionally, SLITRK1 was expressed in medium-spiny neurons also expressing substance P (Fig. 8D–F) and the D<sub>1</sub> dopamine receptor (Fig. 8G–I), established markers of direct pathway striatal neurons projecting to the medial globus pallidus and the substantia nigra, but not in those expressing the indirect pathway marker enkephalin (Gerfen and Young, 1988; Fig. 8J–L). SLITRK1 was further absent from GABA-ergic interneurons, including those expressing PVALB, CALB2, or NOS1 (not shown). Furthermore, SLITRK1 was highly expressed in the globus pallidus, the thalamic parafascicular and lateral dorsal nuclei, and the substantia nigra pars compacta but was absent from the subthalamic nucleus and the substantia nigra pars reticulata, contributing to the overall presence of SLITRK1 in the direct rather than the indirect pathway of the basal ganglia (Fig. 3A–F, and data not shown).

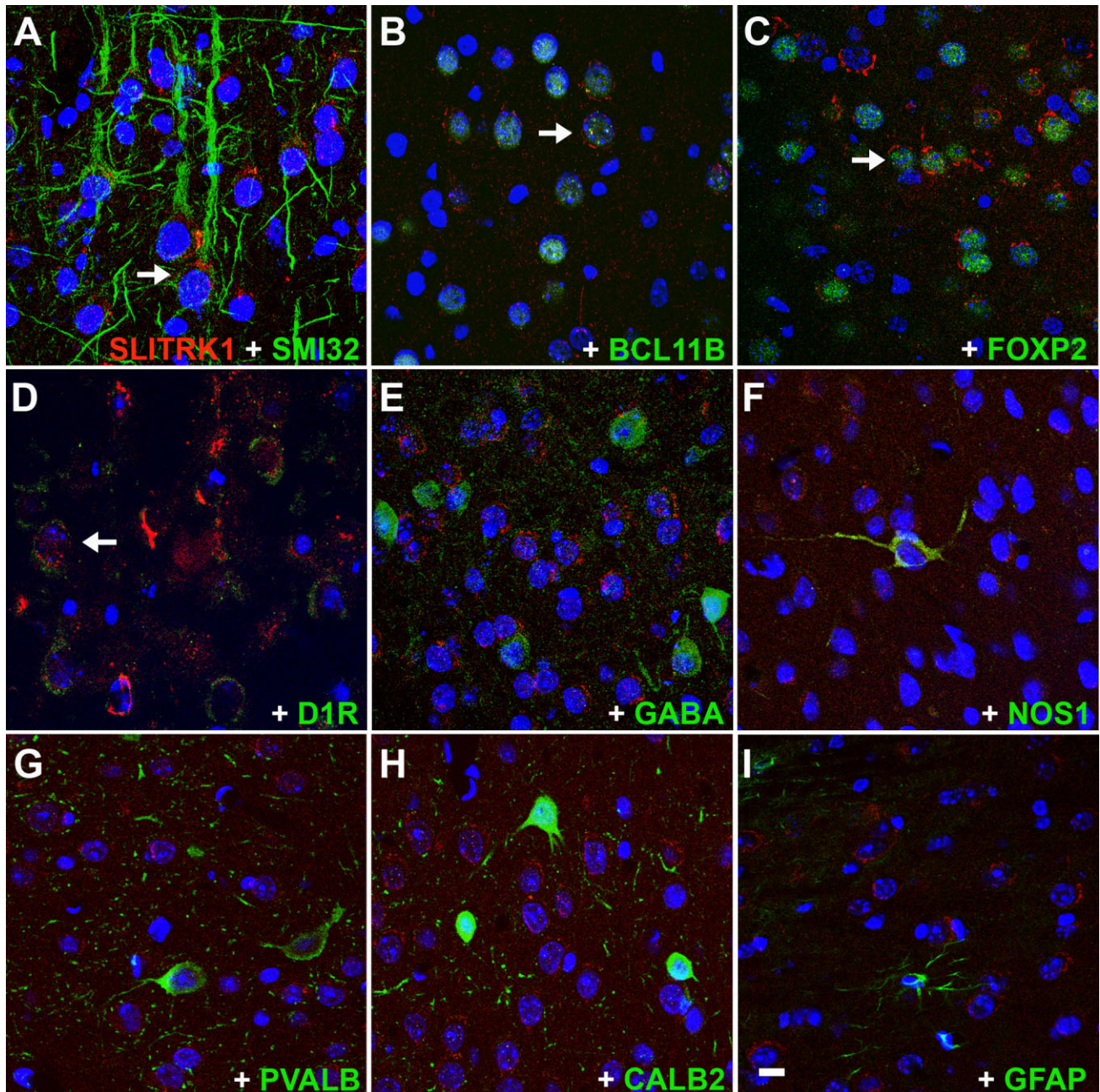


**Figure 5.** SLITRK1 is expressed in cortical projection neurons but not in GABAergic interneurons in P7 mouse brain. Fluorescence confocal analysis of cortical sections immunolabeled with SLITRK1 (in red) and appropriate cell-type-specific markers (in green); cell nuclei are stained with DAPI (in blue). **A–D:** SLITRK1 colocalizes with the following markers: SMI-32, a marker of pyramidal projection neurons (A); BCL11B, a transcription factor found in layer 5 corticospinal and corticotectal neurons (B); and FOXP2, a transcription factor confined to subcortical projection neurons residing predominantly in layer 6 and sparsely in layer 5 (C); partial overlap was also observed with dopamine 1 receptor (D, R; D). **E–H:** No colocalization was observed between SLITRK1 and various interneuron-specific markers, such as GABA, a marker of GABAergic interneurons (E); or with markers of interneuron subtypes, including NOS1 (F), PVALB (G), and CALB2/calretinin (H). **I:** SLITRK1 does not colocalize with the astrocytic marker GFAP. Arrows indicate SLITRK1-expressing neurons (red) that also express the indicated cell-type-specific markers. A magenta-green copy of this figure is included as Supporting Information Figure 2. Scale bar = 10  $\mu$ m.

As mentioned above, a few neurons in the adult striatum appeared to maintain *Slitrk1* mRNA and SLITRK1 protein expression (Fig. 9A–C). These were large, of modest numbers, and scattered throughout the striatum, character-

istics suggesting that they might be giant cholinergic interneurons. Double labeling with anti-SLITRK1 and anti-ChAT antibodies confirmed that in the adult mouse (Fig. 9D), monkey (Fig. 9E), and human (Fig. 9F) striatum, SLITRK1

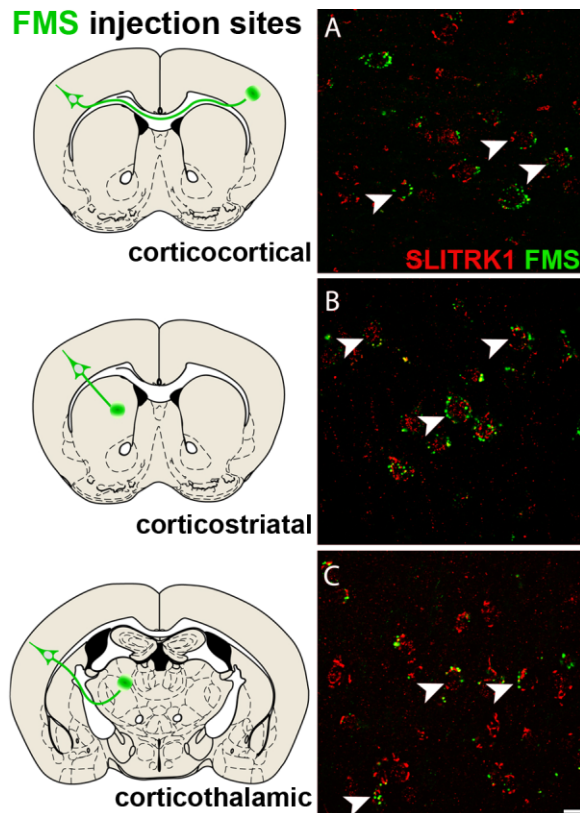


Figure 6. SLITRK1 is expressed in cortical projection neurons of the corticostriatal-thalamocortical circuitry. Retrograde axonal tracing in adult mouse brain using fluorescent microspheres (FMS; green Retro Beads). Diagrams at left indicate the site of microsphere injection (marked by a green circle) and the population of cells examined for the presence of retrogradely transported microspheres (green triangle). A–C: SLITRK1 (red) is present in contralateral corticocortical projection neurons (A) as well as in ipsilateral corticostriatal (B) and corticothalamic (C) projection neurons. Arrowheads indicate retrogradely labeled neurons (green) also expressing SLITRK1 (red). A magenta-green copy of this figure is included as Supporting Information Figure 3. Scale bar = 10  $\mu$ m.

expression was maintained in striatal cholinergic interneurons.

## DISCUSSION

These studies demonstrate that SLITRK1 expression during mammalian brain development is both developmentally regulated and evolutionarily conserved. In the cortex, SLITRK1 is expressed primarily in pyramidal projection neurons and remains confined within the somatodendritic compartment, where its distribution shifts from primarily dendritic to mainly somatic as the brain matures, possibly reflecting a role in the elaboration of apical dendrites. SLITRK1 is associated with cytoplasmic vesicles in both mouse and monkey neocortex, suggesting that it might be secreted. In the striatum, SLITRK1 is transiently expressed in projection neurons of the direct output pathway and concentrated in striosomes during early brain development, consistent with a role in establishing striatal connectivity; expression is maintained only in adult cho-

linergic interneurons. This general pattern is observed in monkey and human brain as well, maintained in cell types and subcellular compartments, with this high degree of conservation suggesting a preserved function of the SLITRK1 protein across mammalian species.

### Potential role for SLITRK1 in cortical dendritic development

SLITRK1 is expressed by cortical pyramidal neurons in layers 3, 5, and 6 in mouse, rhesus monkey, and human brain. These project both intracortically (3) and subcortically (5 and 6) to the striatum and thalamus, thus placing SLITRK1 in the corticostriatal-thalamocortical pathway. SLITRK1 is confined to the somatodendritic compartment, where its distribution is developmentally regulated: early, it is expressed highly in the apical dendrite and at lower levels in the cell body; by the end of the first postnatal week, it appears concentrated in the soma and is detected only at lower levels in the apical dendrite. Within the adult cortical neuronal cell body, SLITRK1 is asymmetrically distributed. These expression patterns are striking; however, the functional implications are presently unknown. Overexpression of SLITRK1 elicits unipolar neurites in cell lines (Aruga and Mikoshiba, 2003) and enhances dendritic branching in primary pyramidal cortical neurons (Abelson et al., 2005). Its enrichment within the apical dendrite as this extends toward the pial surface suggests that SLITRK1 may have a role in dendritic elaboration and integration of information from superficial cortical layers. SLIT/ROBO interactions have been implicated in dendritic patterning (Whitford et al., 2002). Notably, previous work has demonstrated that the oriented outgrowth of the apical dendrite is dependent on asymmetric targeting of a soluble modulator of a chemorepellant/chemoattractant activity (Polleux et al., 2000). Little is known about this process, and subtle imbalances in SLITRK1 distribution within the somatodendritic compartment could affect dendritic integration, possibly changing how signal inputs are processed and transmitted.

### Possible roles for SLITRK1 in striatal circuitry

In the striatum, SLITRK1 is initially broadly expressed, is subsequently concentrated in striosomes in embryonic and early postnatal development, and is undetectable by adulthood, with the notable exception of cholinergic interneurons. During the first 2 postnatal weeks, SLITRK1 appears to be confined to two compartmentalized systems within the striatum: the direct pathway neurons and the striosomes; this segregation possibly implies a functional role for the protein in a subset of developing medium-spiny projection neurons.

Afferent inputs terminate largely on dendritic spines of striatal medium spiny neurons, and, if SLITRK1 is indeed generally involved in dendritic regulation, as suggested by both the effects of its overexpression in primary cortical pyramidal neurons and its localization in the apical cortical dendrite, these terminals may also represent potential sites of SLITRK1 function. Moreover, SLITRK1 may influence dendritic development in the medium-spiny neurons that express it in a manner dependent on nigrostriatal dopaminergic and/or thalamostriatal afferent input. In mouse striatum, dendritic maturation is initiated in the first postnatal week (Sturrock, 1980), a period of high expression of the SLITRK1 protein, in a temporal profile following closely the same process in cortical pyramidal cells (Miller, 1981; Petit et al., 1988).

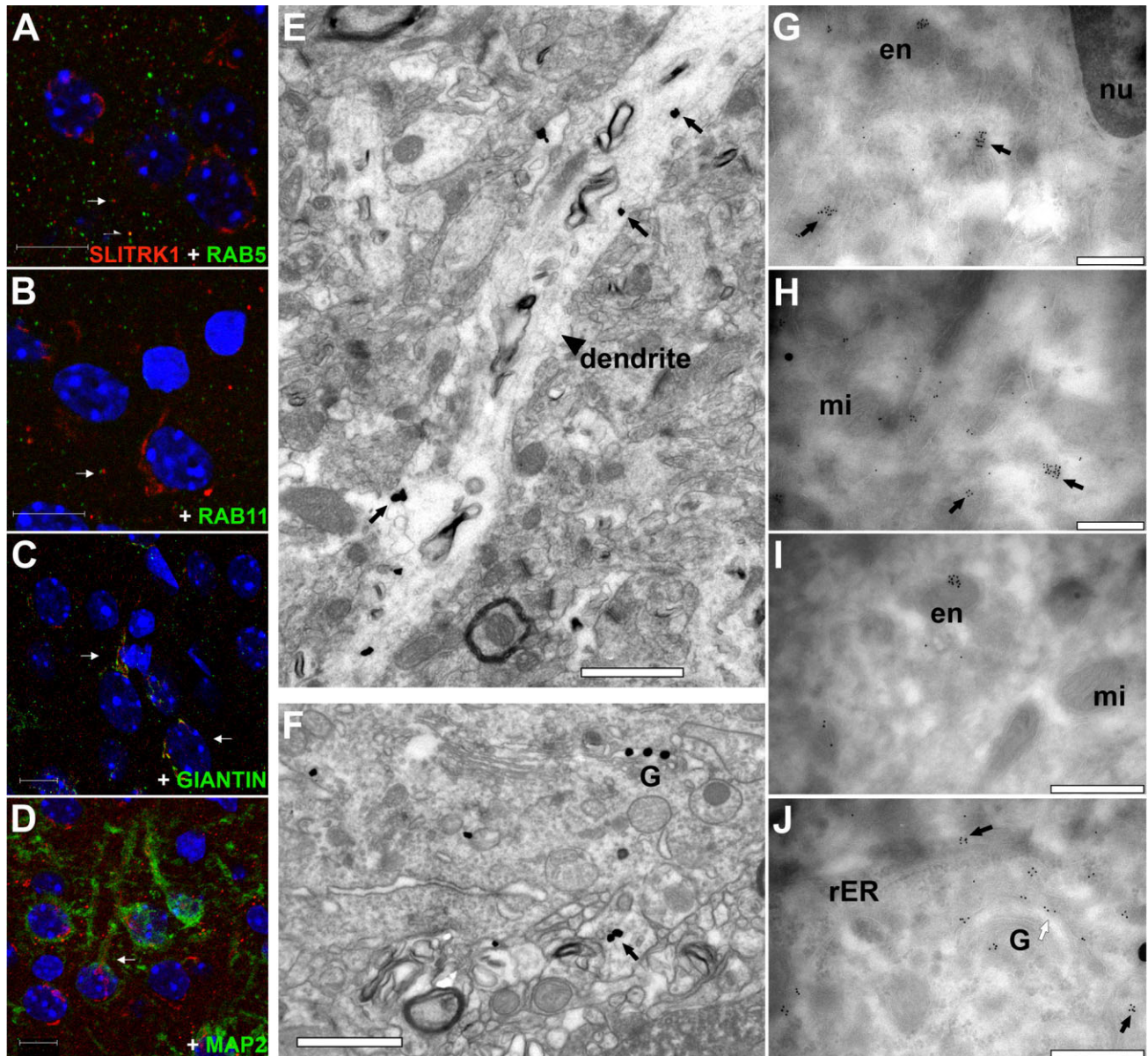


Figure 7.

Subcellular localization of SLITRK1 in cortical neurons. **A–D**: Fluorescence confocal analysis of P7 mouse neocortical sections immunolabeled with SLITRK1 (red) and appropriate subcellular compartment markers (green); cell nuclei are stained with DAPI (blue). Example points of colocalization are indicated by white arrows. SLITRK1 partially colocalizes with RAB5, a marker of early endosomes (A), and overlaps minimally with RAB11, a marker of recycling endosomes (B). SLITRK1 considerably colocalizes with giantin, a marker of the Golgi apparatus (C). SLITRK1 is expressed in the MAP2-labeled apical dendrites of the somatodendritic compartment (D). **E–J**: Immuno-EM localization of SLITRK1 in adult mouse and rhesus monkey cortex. Gold particles are found within cortical dendrites (indicated by a black arrowhead) and cytoplasmic vesicles (black arrows) in the cortex of mouse (E,G–J) and monkey (F). Gold particles are also found within endosomes (en; G,I) as well as in the periphery of the Golgi apparatus (G; F, white arrow in J). SLITRK1 is absent from the nucleus (nu; G), mitochondria (mi; H,I), and rough endoplasmic reticulum (rER; J). A magenta-green copy of this figure is included as Supporting Information Figure 4. Scale bars = 10  $\mu\text{m}$  in A–D; 1  $\mu\text{m}$  in E,F; 500 nm in G–J.

Transient expression of SLITRK1 is restricted to the striosomal (patch) compartment and excluded from the surrounding matrix. Compartments reflect cortical lamination and the segregation of cortical inputs that target different subpopulations of medium-spiny neurons (Gerfen, 1989, 2004), which in turn project to different components of the substantia nigra (SN) and medial globus pallidus (GP). In rodents, for example,

patch and matrix neurons target, respectively, ventral tier dopaminergic (SN pars compacta) and GABAergic neurons (SN pars reticulata); in primates, striatal outputs are not as clearly segregated (Joel and Weiner, 2000; Saka and Graybiel, 2003; Gerfen, 2004).

Furthermore, SLITRK1 is preferentially associated with direct-pathway neurons, projecting to the SN and the medial

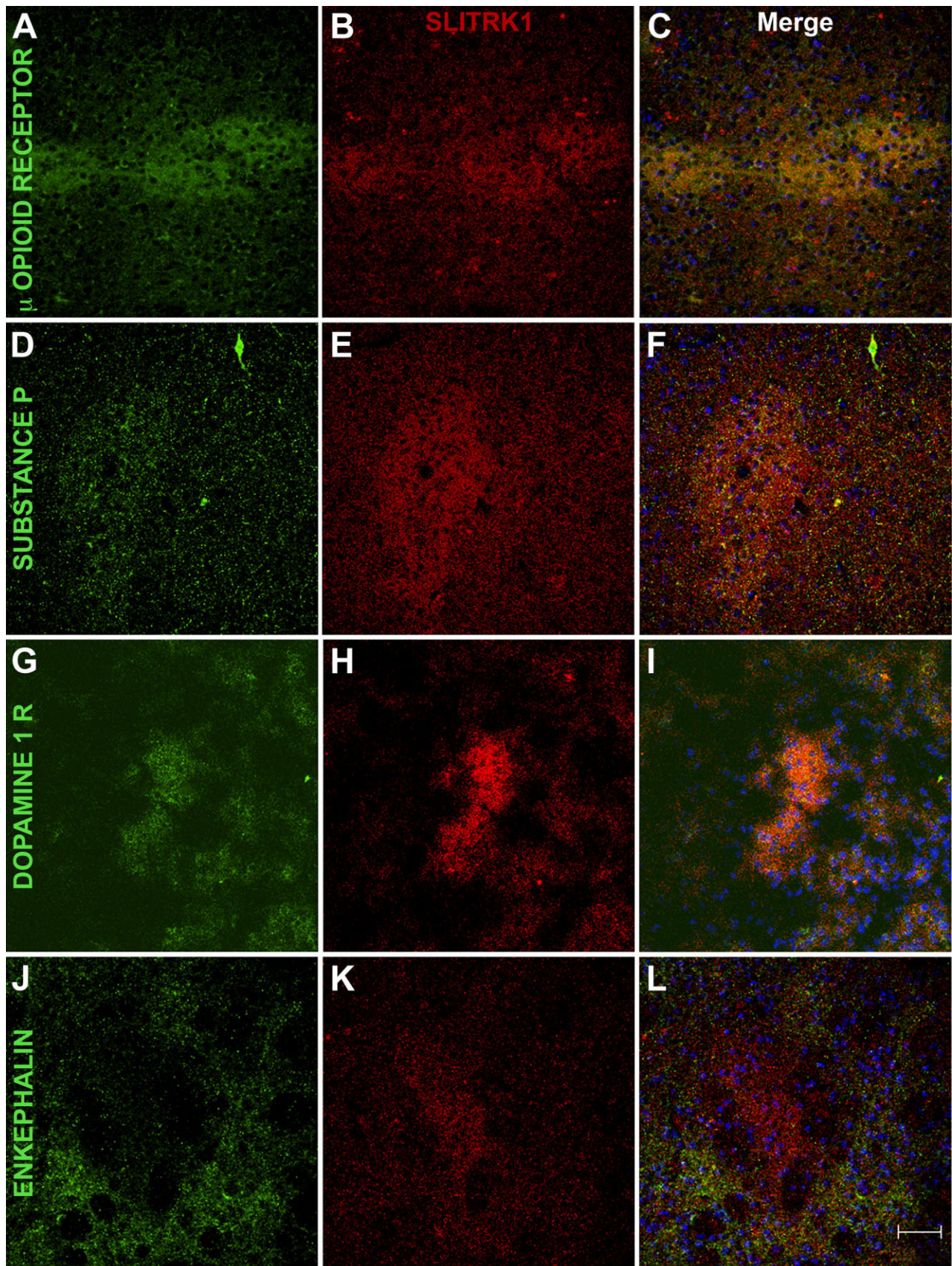
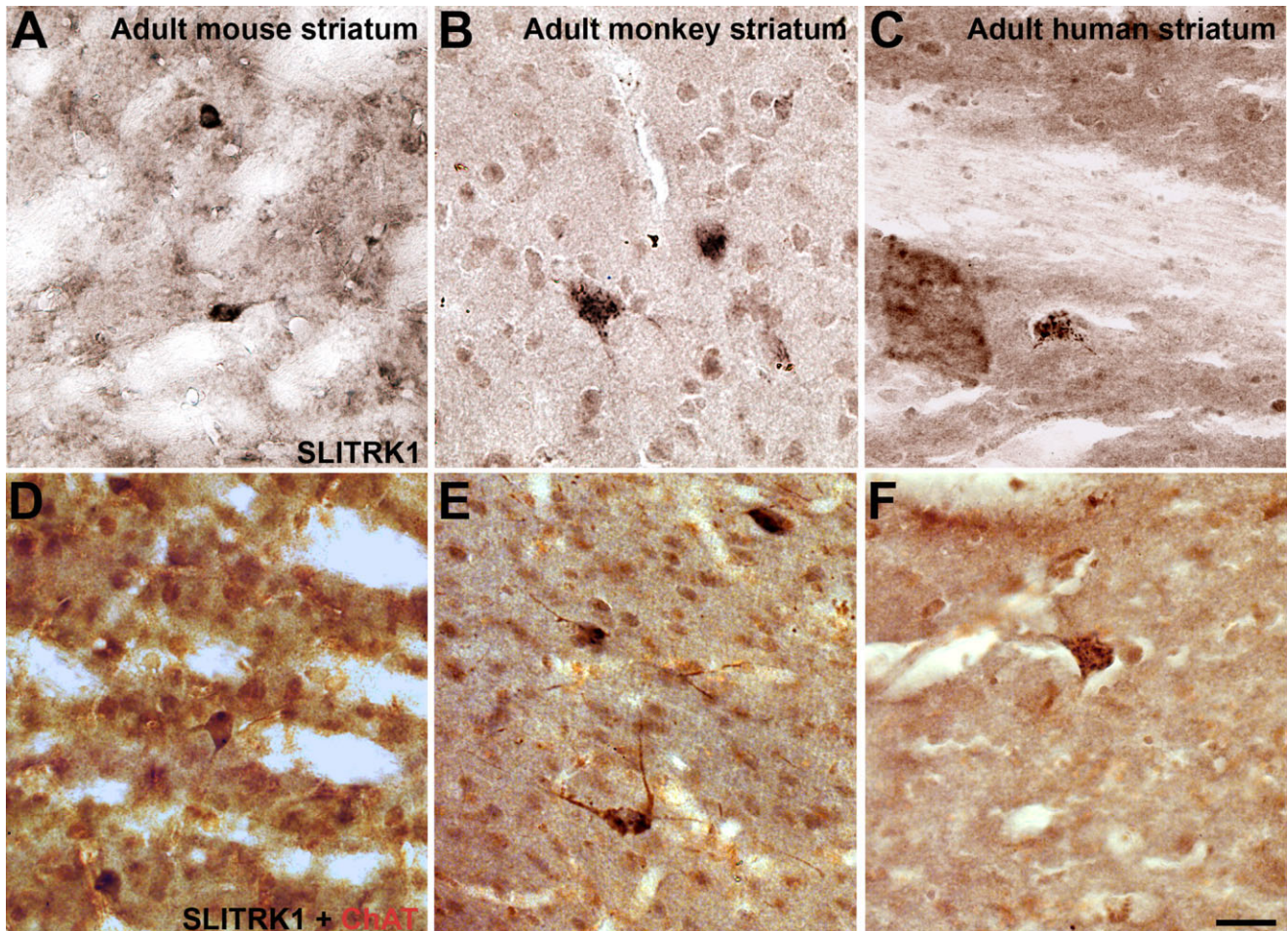


Figure 8. SLITRK1 protein is confined to striosomes and direct pathway neurons in the developing striatum. Fluorescence confocal analysis of P7 mouse brain sections immunolabeled with SLITRK1 (red) and striatal markers (green); cell nuclei are stained with DAPI (blue). A–C: SLITRK1 colocalizes with the  $\mu$ -opioid receptor, a marker of striosomes. D–I: Considerable overlap was observed between SLITRK1 and both substance P (D–F) and dopamine 1 receptor (G–I), both of which are expressed predominantly in direct pathway neurons. J–L: SLITRK1 has a staining pattern reciprocal to that of enkephalin, a marker of indirect pathway neurons. C,F,I,L are merged images of the preceding panels. A magenta-green copy of this figure is included as Supporting Information Figure 5. Scale bar = 50  $\mu$ m.



**Figure 9.** SLITRK1 protein expression is maintained in cholinergic interneurons of adult striatum. Sections of adult mouse, monkey, and human striatum immunolabeled with anti-SLITRK1 (black) and anti-ChAT (red). **A–C:** Representative SLITRK1-positive neurons in adult mouse (A), monkey (B), and human (C) striatum. **D–F:** SLITRK1-positive neurons in adult mouse (D), monkey (E), and human (F) striatum also express ChAT. Cholinergic interneurons are the only cells that express SLITRK1 in the adult striatum. Scale bar = 100  $\mu\text{m}$ .

GP (while also extending collaterals to the lateral GP). In rodents, direct-pathway neurons constitute approximately half of the striatal projection neuron population, are intermingled with indirect neurons (projecting only to the lateral GP) throughout the striatum, and are equally distributed in patches and matrix (Gerfen, 2004). Therefore, SLITRK1 expression appears to define a distinct subset of medium-spiny projection neurons, possibly of distinct function: those segregating within the striosomes and further contributing an axon to the direct pathway.

Finally, adult cholinergic interneurons continue to express SLITRK1; these are thought also to express *Slit1* (Marillat et al., 2002). Although far from being numerous (Rymar et al., 2004), cholinergic interneurons provide very dense local innervation and, unlike most striatal neurons, are autonomous pacemakers spiking in the absence of synaptic activity (Woolf, 1991). They play an important role in the regulation of motor movement (Kaneko et al., 2000), receive dopaminergic input from the SN, and thus lie at the intersection of two extensive and dense local arbors in the striatum, those of cholinergic

interneurons and dopaminergic afferent fibers (Zhou et al., 2002a). Recent experimental and clinical studies have implicated striatal cholinergic interneurons in the induction of synaptic plasticity and motor learning as well as in motor dysfunction, causing a renewed interest in their role in movement disorders (Pisani et al., 2007).

### Implications for TS

TS is characterized by chronic vocal and motor tics that range from simple to complex and by a waxing and waning clinical course (Leckman et al., 2004; Singer, 2005). The onset of TS occurs during childhood, and many patients experience alleviation of symptoms with age, suggesting that the pathway involved is important developmentally (Singer, 2005).

The vast majority of findings with regard to TS pathophysiology have focused attention on the basal ganglia and the corticostriatal-thalamocortical circuitry (Saka and Graybiel, 2003; Albin and Mink, 2006; Leckman et al., 2006a; Singer, 2006). Neuroimaging studies in patients have indicated significantly reduced caudate nucleus volumes (Peterson et al.,

2003), thinning of sensorimotor cortices (Sowell et al., 2008), and high activity in the basal ganglia, thalamus, and corresponding cortical regions during tic suppression (Peterson et al., 1998). However, the underlying molecular and cellular mechanisms are not well understood. Very limited neuropathological and neurotransmitter findings have indicated abnormal dopaminergic innervation of the ventral striatum (Albin et al., 2003), decreased density of striatal dynorphin projections (Haber et al., 1986), and altered distribution of parvalbumin-containing interneurons in the basal ganglia (Kalanithi et al., 2005), but these studies await confirmation.

Two leading hypotheses invoke imbalances in competing basal ganglia circuits as an underlying cause of TS. The first proposes that imbalances in striatal output systems, caused by increased activity of the direct/inhibitory/movement-releasing pathway and concomitant decreased activity of the indirect/disinhibitory/movement-inhibiting pathway, lead to disinhibition of the targeted motor network (Leckman et al., 2006b). The second, based on experimental evidence from rodents and primates, highlights a functional disparity between striosomes and matrix, respectively, more related to motivational behavior and sensorimotor functioning, accompanied by increased activity of the dopaminergic nigrostriatal feedback pathway and abnormalities of dopamine transmission (Saka and Graybiel, 2003). Motor stereotypies induced in rodents by dopaminergic stimulation are accompanied by specific patterns of functional activation, which affect primarily striosomes (Canales and Graybiel, 2000; Capper-Loup et al., 2002). Our findings that SLITRK1 is on one hand preferentially associated with direct pathway neurons, and on the other also expressed in striosomes place it in a position potentially to influence imbalances between either the direct/indirect pathways or the striosomal/matrix compartments.

The specific site of the lesion underlying TS notwithstanding, available evidence from several disciplines, including anatomical and neuroimaging studies, the efficacy of therapeutic agents that interfere with dopaminergic function, and animal models of motor stereotypies, points to abnormalities of dopamine transmission (Saka and Graybiel, 2003; Albin and Mink, 2006). Striatal dopamine and acetylcholine interactions involve both antagonistic balance and also functional cooperativity and are fundamental to striatal function (Cragg, 2006). Several dopamine receptors are expressed by striatal cholinergic interneurons (Nicola et al., 2000; Zhou et al., 2002b), the sole striatal neurons maintaining SLITRK1 expression into adulthood. Furthermore, the changing course of the nigrostriatal dopamine feedback system has been proposed to be associated with tic development in TS (Albin and Mink, 2006): nigrostriatal innervation in the human striatum increases during development, peaking during preadolescence, and has a marked decline toward adulthood (Haycock et al., 2003). It is tempting to speculate that a correlation might exist between this developmental regulation of nigrostriatal innervation and the developmentally regulated expression of SLITRK1 in the striatum.

Regardless of the underlying specific cellular and molecular mechanisms, TS is clearly a developmental disorder. Our previous findings (Abelson et al., 2005) suggest that mutations in *SLITRK1* could have a role in disease, and the present study places SLITRK1 in the neuroanatomical circuits most commonly associated with TS. It is premature to speculate on the

consequences of *SLITRK1* mutations on basal ganglia development and function. The detailed characterization of its highly developmentally regulated and evolutionarily conserved expression, however, points to components of the corticostriatal-thalamocortical pathway that could be affected at specific developmental time points critical for the elaboration of the circuitry.

## ACKNOWLEDGMENTS

We thank Milos Judas and Bradford Poulos for help with tissue acquisition; Carol Nelson-Williams and Kenneth Y. Kwan for advice; Monica Enamandram for technical help; and Yuri Morozov, Christoph Rahner, and the Center for Cell and Molecular Imaging at Yale University School of Medicine for help with electron microscopy.

## LITERATURE CITED

- Abelson JF, Kwan KY, O'Roak BJ, Baek DY, Stillman AA, Morgan TM, Mathews CA, Pauls DL, Rasin MR, Gunel M, Davis NR, Ercan-Sencicek AG, Guez DH, Spertus JA, Leckman JF, Dure LS, Kurlan R, Singer HS, Gilbert DL, Farhi A, Louvi A, Lifton RP, Sestan N, State MW. 2005. Sequence variants in *SLITRK1* are associated with Tourette's syndrome. *Science* 310:317–320.
- Albin RL, Mink JW. 2006. Recent advances in Tourette syndrome research. *Trends Neurosci* 29:175–182.
- Albin RL, Koeppe RA, Bohnen NI, Nichols TE, Meyer P, Wernette K, Minoshima S, Kilbourn MR, Frey KA. 2003. Increased ventral striatal monoaminergic innervation in Tourette syndrome. *Neurology* 61:310–315.
- Ang ES Jr, Haydar TF, Gluncic V, Rakic P. 2003. Four-dimensional migratory coordinates of GABAergic interneurons in the developing mouse cortex. *J Neurosci* 23:5805–5815.
- Arlotta P, Molyneaux BJ, Chen J, Inoue J, Kominami R, Macklis JD. 2005. Neuronal subtype-specific genes that control corticospinal motor neuron development in vivo. *Neuron* 45:207–221.
- Aruga J, Mikoshiba K. 2003. Identification and characterization of *Slitrk*, a novel neuronal transmembrane protein family controlling neurite outgrowth. *Mol Cell Neurosci* 24:117–129.
- Aruga J, Yokota N, Mikoshiba K. 2003. Human *SLITRK* family genes: genomic organization and expression profiling in normal brain and brain tumor tissue. *Gene* 315:87–94.
- Becker KP, Hannun YA. 2003. cPKC-dependent sequestration of membrane-recycling components in a subset of recycling endosomes. *J Biol Chem* 278:52747–52754.
- Berardelli A, Curra A, Fabbrini G, Gilio F, Manfredi M. 2003. Pathophysiology of tics and Tourette syndrome. *J Neurosci* 25:781–787.
- Berg KA, Zardeneta G, Hargreaves KM, Clarke WP, Milam SB. 2007. Integrins regulate opioid receptor signaling in trigeminal ganglion neurons. *Neuroscience* 144:889–897.
- Brandt MD, Jessberger S, Steiner B, Kronenberg G, Reuter K, Bick-Sander A, von der Behrens W, Kempermann G. 2003. Transient calcitonin expression defines early postmitotic step of neuronal differentiation in adult hippocampal neurogenesis of mice. *Mol Cell Neurosci* 24:603–613.
- Britanova O, de Juan Romero C, Cheung A, Kwan KY, Schwark M, Gyorgy A, Vogel T, Akopov S, Mitkovski M, Agoston D, Sestan N, Molnar Z, Tarabykin V. 2008. *Satb2* is a postmitotic determinant for upper-layer neuron specification in the neocortex. *Neuron* 57:378–392.
- Brose K, Bland KS, Wang KH, Arnott D, Henzel W, Goodman CS, Tessier-Lavigne M, Kidd T. 1999. *Slit* proteins bind Robo receptors and have an evolutionarily conserved role in repulsive axon guidance. *Cell* 96:795–806.
- Bruce G, Wainer BH, Hersh LB. 1985. Immunoaffinity purification of human choline acetyltransferase: comparison of the brain and placental enzymes. *J Neurochem* 45:611–620.
- Campbell MJ, Morrison JH. 1989. Monoclonal antibody to neurofilament protein (SMI-32) labels a subpopulation of pyramidal neurons in the human and monkey neocortex. *J Comp Neurol* 282:191–205.
- Canales JJ, Graybiel AM. 2000. A measure of striatal function predicts motor stereotypy. *Nat Neurosci* 3:377–383.

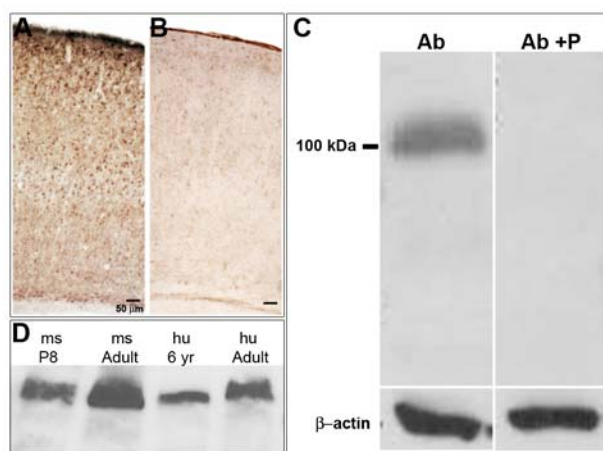
- Capani F, Ellisman MH, Martone ME. 2001. Filamentous actin is concentrated in specific subpopulations of neuronal and glial structures in rat central nervous system. *Brain Res* 923:1–11.
- Capper-Loup C, Canales JJ, Kadaba N, Graybiel AM. 2002. Concurrent activation of dopamine D1 and D2 receptors is required to evoke neural and behavioral phenotypes of cocaine sensitization. *J Neurosci* 22:6218–6227.
- Cataldo AM, Petanceska S, Peterhoff CM, Terio NB, Epstein CJ, Villar A, Carlson EJ, Staufienbiel M, Nixon RA. 2003. App gene dosage modulates endosomal abnormalities of Alzheimer's disease in a segmental trisomy 16 mouse model of down syndrome. *J Neurosci* 23:6788–6792.
- Celio MR, Baier W, Scharer L, de Viragh PA, Gerday C. 1988. Monoclonal antibodies directed against the calcium binding protein parvalbumin. *Cell Calcium* 9:81–86.
- Cragg SJ. 2006. Meaningful silences: how dopamine listens to the ACh pause. *Trends Neurosci* 29:125–131.
- Dotti CG, Banker GA, Binder LI. 1987. The expression and distribution of the microtubule-associated proteins tau and microtubule-associated protein 2 in hippocampal neurons in the rat in situ and in cell culture. *Neuroscience* 23:121–130.
- Fazzari P, Penachioni J, Gianola S, Rossi F, Eickholt BJ, Maina F, Alexopoulou L, Sottile A, Comoglio PM, Flavell RA, Tamagnone L. 2007. Plexin-B1 plays a redundant role during mouse development and in tumour angiogenesis. *BMC Dev Biol* 7:55.
- Ferland RJ, Cherry TJ, Preware PO, Morrisey EE, Walsh CA. 2003. Characterization of *Foxp2* and *Foxp1* mRNA and protein in the developing and mature brain. *J Comp Neurol* 460:266–279.
- Fernandez-Chacon R, Wolfel M, Nishimune H, Tabares L, Schmitz F, Castellano-Munoz M, Rosenmund C, Montesinos ML, Sanes JR, Schleggenburger R, Sudhof TC. 2004. The synaptic vesicle protein CSP alpha prevents presynaptic degeneration. *Neuron* 42:237–251.
- Fuentes-Santamaria V, Alvarado JC, Stein BE, McHaffie JG. 2008. Cortex contacts both output neurons and nitrgic interneurons in the superior colliculus: direct and indirect routes for multisensory integration. *Cereb Cortex* 18:1640–1652.
- Fujimori K, Takauji R, Tamamaki N. 2002. Differential localization of high- and low-molecular-weight variants of microtubule-associated protein 2 in the developing rat telencephalon. *J Comp Neurol* 449:330–342.
- Fujita E, Tanabe Y, Shiota A, Ueda M, Suwa K, Momoi MY, Momoi T. 2008. Ultrasonic vocalization impairment of *Foxp2* (R552H) knockin mice related to speech-language disorder and abnormality of Purkinje cells. *Proc Natl Acad Sci U S A* 105:3117–3122.
- Gabriel R, Witkovsky P. 1998. Cholinergic, but not the rod pathway-related glycinergic (All), amacrine cells contain calretinin in the rat retina. *Neurosci Lett* 247:179–182.
- Garner CC, Tucker RP, Matus A. 1988. Selective localization of messenger RNA for cytoskeletal protein MAP2 in dendrites. *Nature* 336:674–677.
- Gerfen CR. 1989. The neostriatal mosaic: striatal patch-matrix organization is related to cortical lamination. *Science* 246:385–388.
- Gerfen CR. 2004. Basal ganglia. In: Paxinos G, editor. *The rat nervous system*. San Diego: Elsevier.
- Gerfen CR, Young WS 3rd. 1988. Distribution of striatonigral and striatopallidal peptidergic neurons in both patch and matrix compartments: an in situ hybridization histochemistry and fluorescent retrograde tracing study. *Brain Res* 460:161–167.
- Goldstein ME, Sternberger LA, Sternberger NH. 1987. Varying degrees of phosphorylation determine microheterogeneity of the heavy neurofilament polypeptide (Nf-H). *J Neuroimmunol* 14:135–148.
- Grosshans BL, Ortiz D, Novick P. 2006. Rabs and their effectors: achieving specificity in membrane traffic. *Proc Natl Acad Sci U S A* 103:11821–11827.
- Grove EA, Tole S, Limon J, Yip L, Ragsdale CW. 1998. The hem of the embryonic cerebral cortex is defined by the expression of multiple Wnt genes and is compromised in *Gli3*-deficient mice. *Development* 125:2315–2325.
- Haber SN, Kowall NW, Vonsattel JP, Bird ED, Richardson EP Jr. 1986. Gilles de la Tourette's syndrome. A postmortem neuropathological and immunohistochemical study. *J Neurol Sci* 75:225–241.
- Harris K, Singer HS. 2006. Tic disorders: neural circuits, neurochemistry, and neuroimmunology. *J Child Neurol* 21:678–689.
- Haycock JW, Becker L, Ang L, Furukawa Y, Hornykiewicz O, Kish SJ. 2003. Marked disparity between age-related changes in dopamine and other presynaptic dopaminergic markers in human striatum. *J Neurochem* 87:574–585.
- Herkenham M, Pert CB. 1981. Mosaic distribution of opiate receptors, parafascicular projections and acetylcholinesterase in rat striatum. *Nature* 291:415–418.
- Hoekstra PJ, Anderson GM, Limburg PC, Korf J, Kallenberg CG, Minderaa RB. 2004. Neurobiology and neuroimmunology of Tourette's syndrome: an update. *Cell Mol Life Sci* 61:886–898.
- Holt AG, Newman SW. 2004. Distribution of methionine and leucine enkephalin neurons within the social behavior circuitry of the male Syrian hamster brain. *Brain Res* 1030:28–48.
- Hornse H, Banerjee S, Zeitlin H, Robertson M. 2001. The prevalence of Tourette syndrome in 13–14-year-olds in mainstream schools. *J Child Psychol Psychiatry* 42:1035–1039.
- Joel D, Weiner I. 2000. The connections of the dopaminergic system with the striatum in rats and primates: an analysis with respect to the functional and compartmental organization of the striatum. *Neuroscience* 96:451–474.
- Kalanithi PS, Zheng W, Kataoka Y, DiFiglia M, Grantz H, Saper CB, Schwartz ML, Leckman JF, Vaccarino FM. 2005. Altered parvalbumin-positive neuron distribution in basal ganglia of individuals with Tourette syndrome. *Proc Natl Acad Sci U S A* 102:13307–13312.
- Kaneko S, Hikida T, Watanabe D, Ichinose H, Nagatsu T, Kreitman RJ, Pastan I, Nakanishi S. 2000. Synaptic integration mediated by striatal cholinergic interneurons in basal ganglia function. *Science* 289:633–637.
- Katayama K, Yamada K, Ornthanalai VG, Inoue T, Ota M, Murphy NP, Aruga J. 2008. *Slitrk1*-deficient mice display elevated anxiety-like behavior and noradrenergic abnormalities. *Mol Psychiatry* (in press).
- Lai CS, Fisher SE, Hurst JA, Vargha-Khadem F, Monaco AP. 2001. A forkhead-domain gene is mutated in a severe speech and language disorder. *Nature* 413:519–523.
- Lai K, Kaspar BK, Gage FH, Schaffer DV. 2003. Sonic hedgehog regulates adult neural progenitor proliferation in vitro and in vivo. *Nat Neurosci* 6:21–27.
- Leckman JF, Feldman R, Swain JE, Eicher V, Thompson N, Mayes LC. 2004. Primary parental preoccupation: circuits, genes, and the crucial role of the environment. *J Neural Transm* 111:753–771.
- Leckman JF, Bloch MH, Scahill L, King RA. 2006a. Tourette syndrome: the self under siege. *J Child Neurol* 21:642–649.
- Leckman JF, Vaccarino FM, Kalanithi PS, Rothenberger A. 2006b. Annotation: Tourette syndrome: a relentless drumbeat—driven by misguided brain oscillations. *J Child Psychol Psychiatry* 47:537–550.
- Lee WC, Huang H, Feng G, Sanes JR, Brown EN, So PT, Nedivi E. 2006. Dynamic remodeling of dendritic arbors in GABAergic interneurons of adult visual cortex. *PLoS Biol* 4:e29.
- Levey AI, Hersch SM, Rye DB, Sunahara RK, Niznik HB, Kitt CA, Price DL, Maggio R, Brann MR, Ciliax BJ, et al. 1993. Localization of D1 and D2 dopamine receptors in brain with subtype-specific antibodies. *Proc Natl Acad Sci U S A* 90:8861–8865.
- Li HS, Chen JH, Wu W, Fagaly T, Zhou L, Yuan W, Dupuis S, Jiang ZH, Nash W, Gick C, Ornitz DM, Wu JY, Rao Y. 1999. Vertebrate slit, a secreted ligand for the transmembrane protein roundabout, is a repellent for olfactory bulb axons. *Cell* 96:807–818.
- Linstedt AD, Hauri HP. 1993. Giantin, a novel conserved Golgi membrane protein containing a cytoplasmic domain of at least 350 kDa. *Mol Biol Cell* 4:679–693.
- Lysakowski A, Wainer BH, Bruce G, Hersh LB. 1989. An atlas of the regional and laminar distribution of choline acetyltransferase immunoreactivity in rat cerebral cortex. *Neuroscience* 28:291–336.
- Marillat V, Cases O, Nguyen-Ba-Charvet KT, Tessier-Lavigne M, Sotelo C, Chedotal A. 2002. Spatiotemporal expression patterns of slit and robo genes in the rat brain. *J Comp Neurol* 442:130–155.
- Miller M. 1981. Maturation of rat visual cortex. I. A quantitative study of Golgi-impregnated pyramidal neurons. *J Neurocytol* 10:859–878.
- Morgado-Valle C, Feldman JL. 2004. Depletion of substance P and glutamate by capsaicin blocks respiratory rhythm in neonatal rat in vitro. *J Physiol* 555:783–792.
- Nicola SM, Surmeier J, Malenka RC. 2000. Dopaminergic modulation of neuronal excitability in the striatum and nucleus accumbens. *Annu Rev Neurosci* 23:185–215.
- Peterson BS, Skudlarski P, Anderson AW, Zhang H, Gatenby JC, Lacadie CM, Leckman JF, Gore JC. 1998. A functional magnetic resonance imaging study of tic suppression in Tourette syndrome. *Arch Gen Psychiatry* 55:326–333.
- Peterson BS, Thomas P, Kane MJ, Scahill L, Zhang H, Bronen R, King RA,

- Leckman JF, Staib L. 2003. Basal ganglia volumes in patients with Gilles de la Tourette syndrome. *Arch Gen Psychiatry* 60:415–424.
- Petit TL, LeBoutillier JC, Gregorio A, Libstug H. 1988. The pattern of dendritic development in the cerebral cortex of the rat. *Brain Res* 469:209–219.
- Pisani A, Bernardi G, Ding J, Surmeier DJ. 2007. Re-emergence of striatal cholinergic interneurons in movement disorders. *Trends Neurosci* 30:545–553.
- Pla R, Borrell V, Flames N, Marin O. 2006. Layer acquisition by cortical GABAergic interneurons is independent of Reelin signaling. *J Neurosci* 26:6924–6934.
- Polleux F, Morrow T, Ghosh A. 2000. Semaphorin 3A is a chemoattractant for cortical apical dendrites. *Nature* 404:567–573.
- Rakic P, Goldman-Rakic PS. 1985. Use of fetal neurosurgery for experimental studies of structural and functional brain development in non-human primates. In: Thomson RA, Green JR, Johnsen SD, editors. *Perinatal neurology and neurosurgery*. New York: Spectrum. p 1–15.
- Rasin MR, Gazula VR, Breunig JJ, Kwan KY, Johnson MB, Liu-Chen S, Li HS, Jan LY, Jan YN, Rakic P, Sestan N. 2007. Numb and Numb1 are required for maintenance of cadherin-based adhesion and polarity of neural progenitors. *Nat Neurosci* 10:819–827.
- Ren Z, Riley NJ, Garcia EP, Sanders JM, Swanson GT, Marshall J. 2003. Multiple trafficking signals regulate kainate receptor KA2 subunit surface expression. *J Neurosci* 23:6608–6616.
- Robertson MM. 2003. Diagnosing Tourette syndrome: is it a common disorder? *J Psychosom Res* 55:3–6.
- Rymar VV, Sasseville R, Luk KC, Sadikot AF. 2004. Neurogenesis and stereological morphometry of calretinin-immunoreactive GABAergic interneurons of the neostriatum. *J Comp Neurol* 469:325–339.
- Saka E, Graybiel AM. 2003. Pathophysiology of Tourette's syndrome: striatal pathways revisited. *Brain Dev* 25(Suppl 1):S15–S19.
- Singer HS. 2005. Tourette's syndrome: from behaviour to biology. *Lancet Neurol* 4:149–159.
- Singer HS. 2006. Discussing outcome in Tourette syndrome. *Arch Pediatr Adolesc Med* 160:103–105.
- Singer HS, Minzer K. 2003. Neurobiology of Tourette's syndrome: concepts of neuroanatomic localization and neurochemical abnormalities. *Brain Dev* 25(Suppl 1):S70–S84.
- Sowell ER, Kan E, Yoshii J, Thompson PM, Bansal R, Xu D, Toga AW, Peterson BS. 2008. Thinning of sensorimotor cortices in children with Tourette syndrome. *Nat Neurosci* 11:637–639.
- Spiteri E, Konopka G, Coppola G, Bomar J, Oldham M, Ou J, Vernes SC, Fisher SE, Ren B, Geschwind DH. 2007. Identification of the transcriptional targets of FOXP2, a gene linked to speech and language, in developing human brain. *Am J Hum Genet* 81:1144–1157.
- State MW, Pauls DL, Leckman JF. 2001. Tourette's syndrome and related disorders. *Child Adolesc Psychiatr Clin N Am* 10:317–331, ix.
- Sturrock RR. 1980. A comparative quantitative and morphological study of ageing in the mouse neostriatum, indusium griseum and anterior commissure. *Neuropathol Appl Neurobiol* 6:51–68.
- Sun YG, Chen ZF. 2007. A gastrin-releasing peptide receptor mediates the itch sensation in the spinal cord. *Nature* 448:700–703.
- Tole S, Patterson PH. 1995. Regionalization of the developing forebrain: a comparison of FORSE-1, Dlx-2, and BF-1. *J Neurosci* 15:970–980.
- Topark-Ngarm A, Golonzka O, Peterson VJ, Barrett B Jr, Martinez B, Crofoot K, Filtz TM, Leid M. 2006. CTIP2 associates with the NuRD complex on the promoter of p57KIP2, a newly identified CTIP2 target gene. *J Biol Chem* 281:32272–32283.
- Whitford KL, Marillat V, Stein E, Goodman CS, Tessier-Lavigne M, Chedotal A, Ghosh A. 2002. Regulation of cortical dendrite development by Slit-Robo interactions. *Neuron* 33:47–61.
- Woolf NJ. 1991. Cholinergic systems in mammalian brain and spinal cord. *Prog Neurobiol* 37:475–524.
- Yung KK, Bolam JP, Smith AD, Hersch SM, Ciliax BJ, Levey AI. 1995. Immunocytochemical localization of D1 and D2 dopamine receptors in the basal ganglia of the rat: light and electron microscopy. *Neuroscience* 65:709–730.
- Zheng H, McKay J, Buss JE. 2007. H-Ras does not need COP I- or COP II-dependent vesicular transport to reach the plasma membrane. *J Biol Chem* 282:25760–25768.
- Zhou FC, Lesch KP, Murphy DL. 2002a. Serotonin uptake into dopamine neurons via dopamine transporters: a compensatory alternative. *Brain Res* 942:109–119.
- Zhou FM, Wilson CJ, Dani JA. 2002b. Cholinergic interneuron characteristics and nicotinic properties in the striatum. *J Neurobiol* 53:590–605.
- Zimmermann L, Schwaller B. 2002. Monoclonal antibodies recognizing epitopes of calretinins: dependence on Ca<sup>2+</sup>-binding status and differences in antigen accessibility in colon cancer cells. *Cell Calcium* 31:13–25.

## Supporting Information

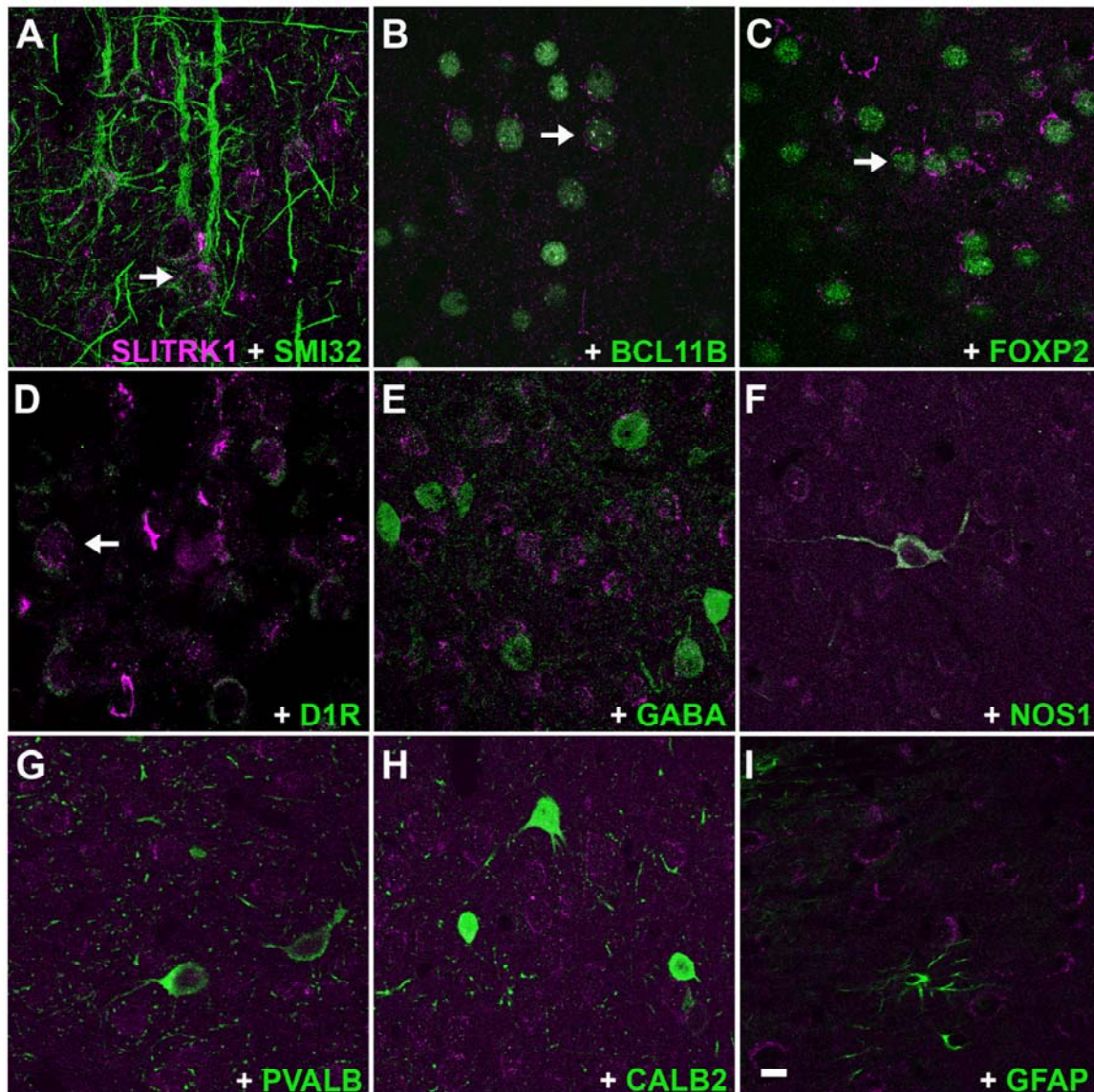
### Developmentally Regulated and Evolutionarily Conserved Expression of SLITRK1 in Brain Circuits Implicated in Tourette Syndrome

Stillman AA, Krsnik Z, Sun J, Rasin MR, State MW, Sestan N, Louvi A

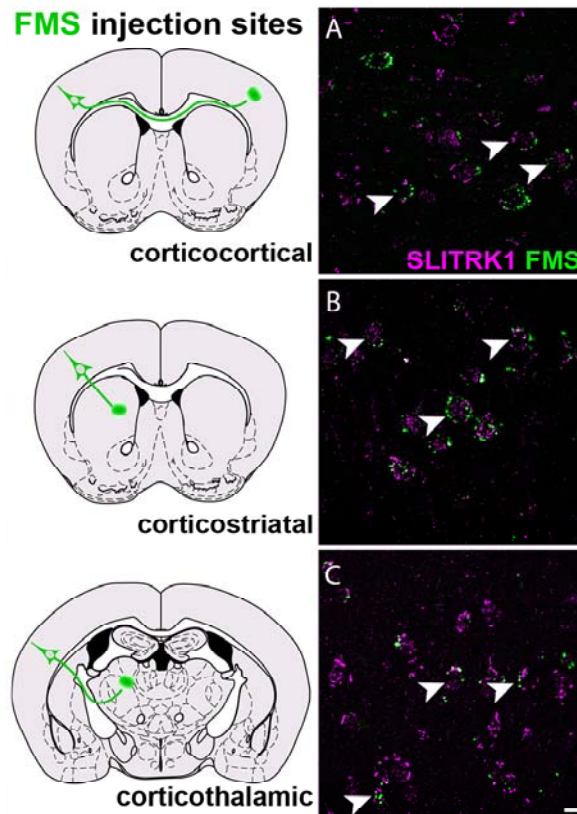


#### Supplementary Figure 1.

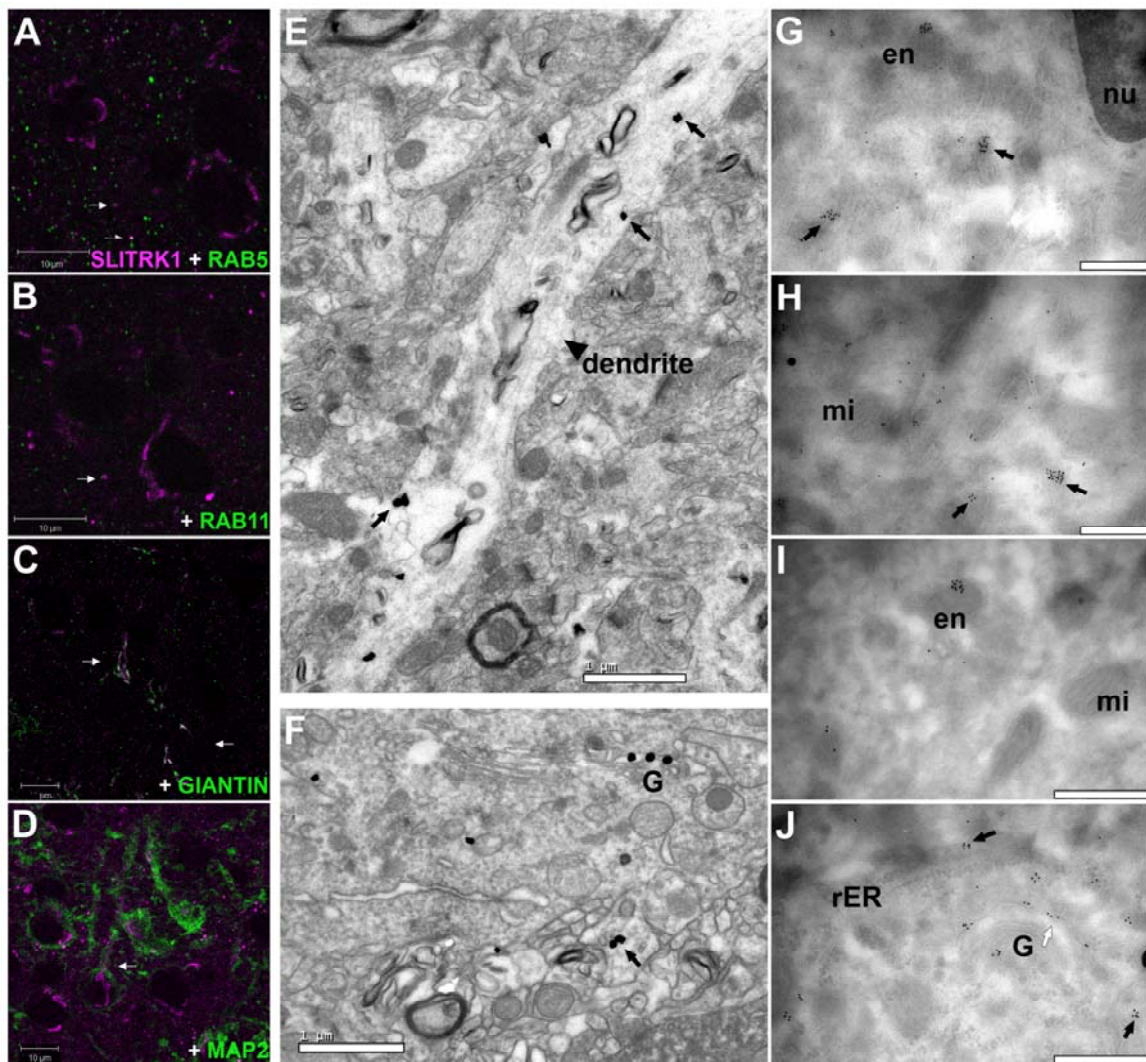
SLITRK1 antibody characterization. **A, B:** P7 mouse cortex immunostained with anti-SLITRK1 (A), or with the antibody pre-incubated with the immunizing peptide (recombinant human SLITRK1 extracellular domain) (B). **C:** On Western blots of mouse brain protein extracts the antibody (Ab) detected a 100 kD m.w. band that was abolished following antibody pre-incubation with the antigenic peptide (Ab+P). β-actin is shown at the bottom as a loading control. **D:** On Western blots of protein extracts from mouse brain (early postnatal [P8] and adult) and human cortex (6 years of age and adult) the antibody recognized only the expected band of 100 kD m.w. in all samples. Scale bar = 50 μm (in A, B).



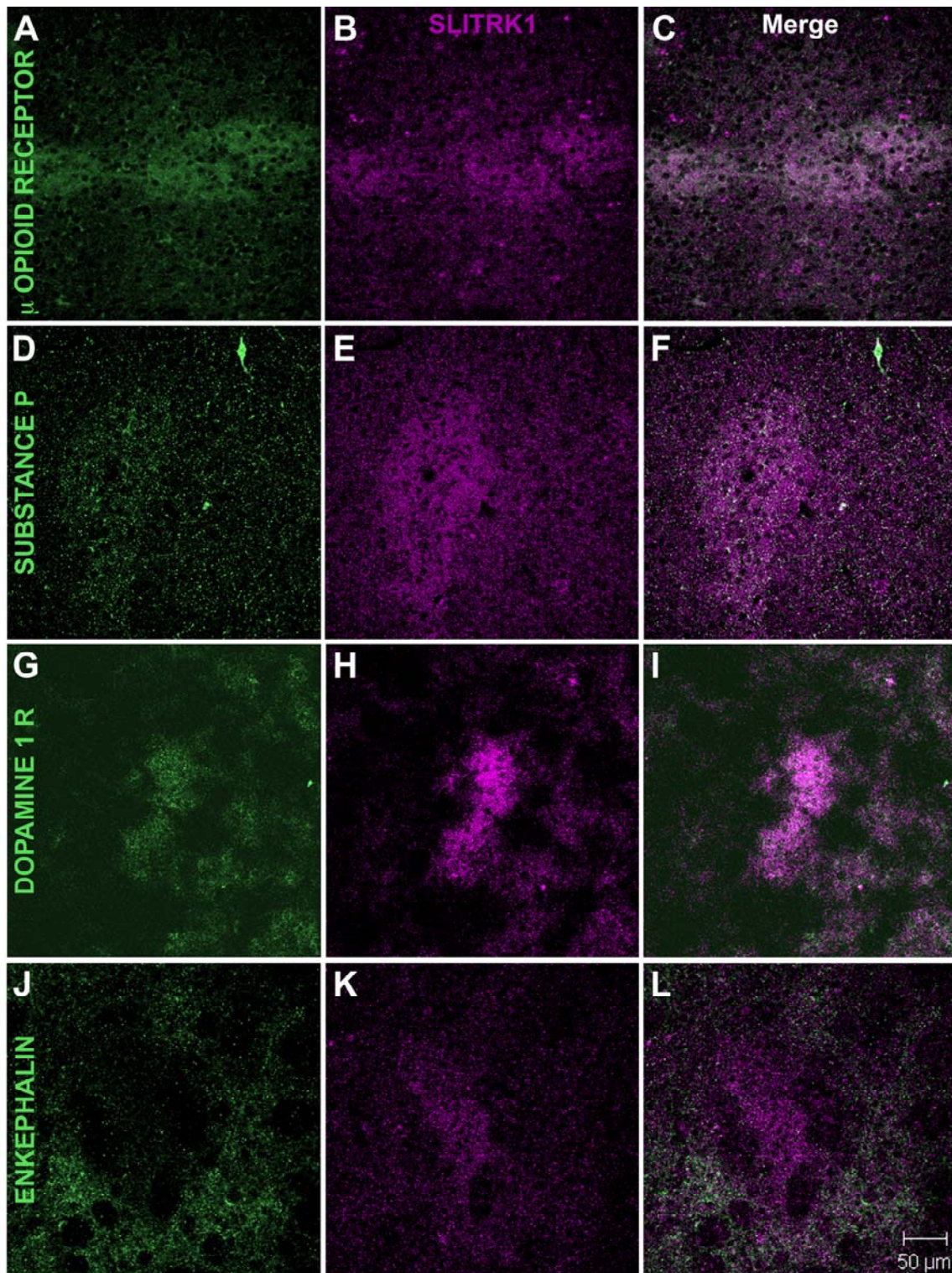
**Supplementary Figure 2**  
Magenta-green version of text figure 5.



**Supplementary Figure 3**  
Magenta-green version of text figure 6.



**Supplementary Figure 4**  
Magenta-green version of text figure 7.



**Supplementary Figure 5**  
Magenta-green version of text figure 8.